

EFFECTS OF MAGNETOSTRICTION AND SUPERLATTICE FORMATION  
IN FERROMAGNETIC THIN FILMS

Thesis by

Gordon O. Johnson

In Partial Fulfillment of the Requirements  
for the Degree of  
Doctor of Philosophy

California Institute of Technology  
Pasadena, California

1972

(Submitted March 16, 1972)

## ACKNOWLEDGMENTS

I wish to thank Professor C. H. Wilts and Professor F. B. Humphrey for their patient assistance and encouragement during the course of this study. Many conversations with L. W. Brownlow also proved to be extremely helpful. The secretarial assistance of K. Ellison was invaluable, and the technical assistance of E. Mott was greatly appreciated. Financial support from a NASA Traineeship, an NSF Fellowship, a Ford Foundation Fellowship, and two teaching assistantships made my stay at Caltech possible. The encouragement and support of my wife, Pat, helped to make this a reality.

## ABSTRACT

The contribution to the magnetic uniaxial perpendicular anisotropy which arises from substrate constraint through magnetostrictive effects has been measured in Ni-Fe and Ni-Co thin films evaporated on substrates at room temperature. This was accomplished by measuring the perpendicular anisotropy before and after removal of the film from the substrate. Data are given for the fcc crystal structure regions of both alloy systems, but data for Ni-Co include compositions with less than 60% Ni which have a small percentage of the hcp phase mixed with the fcc phase. The constraint contribution to the perpendicular anisotropy correlates well with the value of the bulk magnetostriction constant using the equation  $\Delta K_{\perp} = \frac{3}{2} \lambda_s \sigma$ . Measured values of isotropic stress for films thicker than 600 Å were  $1.6 \times 10^{10}$  dyn/cm<sup>2</sup>. In films less than 600 Å thick the isotropic stress decreased with decreasing thickness. After removal of the films from the substrates, the measured perpendicular anisotropy deviated from the expected geometrical shape anisotropy near pure Ni in both alloys. This indicates that additional significant sources of anisotropy exist at these compositions.

The effect of substrate constraint on the crystalline anisotropy  $K_{\perp}$  of Ni-Fe epitaxial films has been studied by use of a film removal technique, which involves the evaporation of an epitaxial layer of LiF on MgO, the epitaxial growth of the metallic film on the LiF, and the stripping of the film with water soluble tape. Films ranging in composition from 50% to 100% Ni have been studied. For compositions below 90% Ni the experimental values agree reasonably well with the first

order theoretical prediction,  $\Delta K_1 = [-\frac{9}{4} (C_{11} - C_{12}) \lambda_{100}^2 + \frac{9}{2} C_{44} \lambda_{111}^2]$ .

In order to compare the magnetic properties of epitaxial thin films more completely with the properties of bulk single crystals, Ni-Fe films ranging in composition from 60% to 90% Ni, which were evaporated epitaxially on (100) MgO substrates, have been subsequently annealed at 400°C in a vacuum of less than  $10^{-7}$  Torr to form the ordered Ni<sub>3</sub>Fe structure near the 75% composition. This ordered structure has been confirmed by electron diffraction.

The saturation magnetization at Ni<sub>3</sub>Fe increased about 6% with ordering which is in good agreement with previous bulk data. Measurements of the magnetocrystalline anisotropy energy  $K_1$  for the epitaxial films show the same large changes with ordering as observed in bulk single crystal samples. In the (001) plane the magnetostriction constants  $\lambda_{100}$ ,  $\lambda_{111}$  are directly related to the induced anisotropy due to a uniform uniaxial strain in the [100] and [110] directions respectively. Assuming that the elastic constants of a film are the same as in bulk material and are unchanged by ordering, the changes in strain sensitivity with ordering for the epitaxial films are found to be in good agreement with values predicted from bulk data. The exchange constant A as measured by ferromagnetic resonance has been measured at the Ni<sub>3</sub>Fe composition and found to increase 25% with ordering. This seems to indicate a significant increase in the Curie temperature which has only been inferred indirectly for bulk material.

## TABLE OF CONTENTS

ACKNOWLEDGMENTS		ii
ABSTRACT		iii
TABLE OF CONTENTS		v
Chapter 1	PERPENDICULAR ANISOTROPY IN POLYCRYSTALLINE THIN FILMS OF Ni-Fe AND Ni-Co	1
	1.1 <u>Introduction</u>	1
	1.2 <u>Theory</u>	3
	1.3 <u>Experimental Methods</u>	4
	1.4 <u>Results and Discussion</u>	7
	1.4.1 Comparison of Stress Dependent Perpendicular Anisotropy With Theory	7
	1.4.2 Evidence for Another Source of Perpendicular Anisotropy	13
Chapter 2	EFFECT OF SUBSTRATE CONSTRAINT ON THE CRYSTALLINE ANISOTROPY OF EPITAXIAL FILMS	18
	2.1 <u>Introduction</u>	18
	2.2 <u>Theory</u>	20
	2.3 <u>Experimental Methods</u>	23
	2.4 <u>Results and Discussion</u>	25
Chapter 3	FORMATION OF ORDERED Ni <sub>3</sub> Fe AND ITS EFFECTS ON THE PROPERTIES OF Ni-Fe THIN FILMS	31
	3.1 <u>Introduction</u>	31

	3.2 <u>Experimental Methods and Theoretical</u>	
	<u>Predictions</u>	32
	3.3 <u>Confirmation of Ni<sub>3</sub>Fe Structure</u>	37
	3.4 <u>Results</u>	39
	3.4.1 Effect of Ordering on Saturation	
	Magnetization	39
	3.4.2 Effect of Ordering on K <sub>1</sub>	41
	3.4.3 Effect of Ordering on Strain	
	Sensitivity	45
	3.5 <u>Discussion</u>	49
Chapter 4	EFFECT OF ORDERING ON THE EXCHANGE CONSTANT A	55
	4.1 <u>Introduction</u>	55
	4.2 <u>Experimental Methods</u>	59
	4.3 <u>Results</u>	61
	4.4 <u>Discussion</u>	65
Appendix 1	STRAIN SENSITIVITY OF SINGLE CRYSTALS	68
Appendix 2	STRAIN SENSITIVITY BASED ON ISOTROPIC MATERIAL	
	MODEL	71
REFERENCES		74

## Chapter 1

## PERPENDICULAR ANISOTROPY IN POLYCRYSTALLINE THIN FILMS

## OF Ni-Fe AND Ni-Co

1.1 Introduction

There are two general types of magnetic anisotropy which are observed in polycrystalline ferromagnetic thin films. The first type is an in-plane uniaxial anisotropy which is made evident when the magnetization rotates in the film plane. The energy density associated with this anisotropy is generally small in size, on the order of  $10^4$  ergs/cm<sup>3</sup>. The sources of this anisotropy have been sought for over a decade because of the potential use of magnetic films for computer memories. One component is almost certainly associated with magnetoelastic effects, but no clear picture has yet emerged. The other general type of anisotropy is a perpendicular uniaxial anisotropy which is made evident when the magnetization is rotated out of the plane of the film. This anisotropy is much larger than the in-plane anisotropy and is on the order of  $10^5$  to  $10^6$  ergs/cm<sup>3</sup>. Until recent developments in bubble domain memories there was no great interest in a detailed understanding of the perpendicular anisotropy. The geometrical shape anisotropy has long been recognized as one source of this anisotropy, but no comprehensive study of the contribution of magnetostrictive effects has been made.

In this study the contribution to the uniaxial perpendicular anisotropy which arises from substrate constraint through magnetostrictive

effects has been measured over the entire Ni-Co and Ni-Fe alloy systems. The isotropic stress in a thin film has previously been shown to contribute to the perpendicular anisotropy through magnetostrictive effects, but only in the case of pure Ni films has a quantitative correlation been shown to exist between the stress and the anisotropy (Fujiwara and Sugita, 1968; Koikeda et al., 1966; Klokholm and Freedman, 1967). To predict quantitatively the magnetostrictive contribution to the perpendicular anisotropy, it is necessary to know the value of the isotropic stress in the plane of the film. Several authors (Klokholm, 1965; Riesenfeld, 1965; Hoffman, 1966) have reported values of isotropic stress in thin films measured by means of a bending beam or plate. These data are for films of Ni, Fe, and alloy compositions near 80 Ni-20 Fe. The results from different laboratories are in poor agreement, but the isotropic stress for films evaporated on substrates at room temperature seems to show little dependence on composition and thickness up to 3000 Å. The reported stresses are all tensile and have an average value of about  $1 \times 10^{10}$  dyn/cm<sup>2</sup>.

The effective anisotropy normal to the film surface includes the shape anisotropy and perpendicular anisotropy due to other sources. In this study ferromagnetic resonance techniques have been used to measure the effective perpendicular anisotropy field in thin films before and after removal of the films from the substrates. The film removal technique was developed by Brownlow and Wilts (1970) in a study of substrate constraint contributions to the in-plane anisotropy. Assuming that the shape anisotropy does not change when the film is removed from the

substrate, any difference in effective perpendicular anisotropy field will be a measure of the change in the perpendicular anisotropy due to substrate constraint.

## 1.2 Theory

If an isotropic stress exists in the plane of an otherwise unconstrained magnetic thin film, it should result in a perpendicular anisotropy energy

$$K_{\perp} = -\frac{3}{2} \lambda_s \sigma, \quad (1.1)$$

where  $\lambda_s$  is the longitudinal saturation magnetostriction constant and  $\sigma$  is the isotropic stress with a positive  $\sigma$  indicating tension (Bozorth, 1951). This energy is just that energy which is required to rotate the magnetization from an in-plane orientation to a position perpendicular to the plane, under the constraint that the in-plane isotropic stress remains at a constant value. Because of magnetostrictive effects a film which is rigidly attached to a substrate is no longer in a condition of constant isotropic stress in the plane but rather in the condition of constant isotropic strain in the plane and zero stress perpendicular. However the saturation magnetostrictive strain is less than 1% of the experimentally observed isotropic strain, so Eq. (1.1) should hold for this case also.

The effective anisotropy energy can be calculated from a ferromagnetic resonance measurement of the perpendicular anisotropy field  $H_{k_{\perp}}$ , since they are related by  $H_{k_{\perp}} = 2(K_{\perp}/M_s)$ , where  $M_s$  is the saturation magnetization. The condition for perpendicular resonance (dc

magnetic field normal to film plane) is taken to be

$$\frac{\omega}{\gamma} = H_{a\perp} - (4\pi M_s - H_{k\perp}), \quad (1.2)$$

where  $\omega$  is the resonant frequency,  $\gamma$  the gyromagnetic ratio, and  $H_{a\perp}$  the applied dc magnetic field normal to the film surface. The contribution due to exchange is neglected for reasons to be discussed later.

The condition for parallel resonance (dc magnetic field parallel to film plane) is taken to be

$$\left(\frac{\omega}{\gamma}\right)^2 = H_{a\parallel} [H_{a\parallel} + (4\pi M_s - H_{k\perp})], \quad (1.3)$$

where  $H_{a\parallel}$  is the applied dc magnetic field in the film plane. The usual in-plane uniaxial anisotropy field can be ignored in both perpendicular and parallel resonance since it is much smaller than the perpendicular anisotropy fields.

### 1.3 Experimental Methods

All samples were made in an oil diffusion pump vacuum system at pressures of about  $10^{-7}$  Torr. An induction heater was used to evaporate the films from 20 gram slugs of material which were in alumina crucibles. The substrates were 1.2 cm square pieces of Corning 0211 glass about 0.5 mm thick. The slides were cleaned ultrasonically in a chromic acid cleaning solution, acetone, and distilled water. Four samples were made simultaneously, one on a cleaned glass slide and three on cleaned glass slides coated with a thin layer of a water soluble polymer, polyvinyl pyrrolidone. Since the polyvinyl pyrrolidone evaporates at about  $150^\circ\text{C}$  in the vacuum, no attempt was made to outgas

the substrates except to keep them in the vacuum for about a half hour at room temperature before the films were evaporated. Film thicknesses ranged from 100 to 4000 Å. The weight percentage composition of the samples was found by X-ray fluorescence. The sample on the uncoated substrate was used as a check to insure that the effective perpendicular anisotropy field of the samples on coated substrates was in good agreement with that of the samples on glass. The samples on the coated substrates could then be removed from the substrates by allowing a water drop to migrate under the sample. Since the water would evaporate in a few minutes, glycerin was substituted for the water in some cases in order to permit magnetic measurements while the samples were freely floating on the surface of the liquid.

Ferromagnetic resonance was detected by measuring transmission through a stripline in which the ferromagnetic samples were inserted (Patton, 1968). Frequencies ranged from 2 to 8 GHz. Parallel resonance measurements could be made over the entire Ni-Fe and Ni-Co alloy ranges, whereas perpendicular resonance measurements were restricted to compositions above 60 wt. % Ni in the Ni-Fe alloys and above 35 wt. % Ni in the Ni-Co alloys because of the 16-kG limitation in the available magnetic field. In the early stages of this investigation, films removed from the substrate were measured by parallel resonance which allowed the film to be in a horizontal position while freely floating on glycerin. Perpendicular resonance, which required the films to be in a vertical position, was performed by floating the films on water and picking them up on clean glass slides. As the water evaporated, the films settled

on the substrates. Both methods of sample treatment gave indistinguishable results; therefore, the films, after settling back onto the substrates, must be in a condition of low strain. The second method was used for both parallel and perpendicular resonance measurements in the later stages of the investigation, since samples handled in this way were less subject to accidental damage.

The effective perpendicular anisotropy field ( $4\pi M_s - H_{k\perp}$ ) can be measured in principle using either perpendicular or parallel resonance. Using the perpendicular resonance condition given in the previous section, the field ( $4\pi M_s - H_{k\perp}$ ) can be obtained by the extrapolation to zero frequency of a graph of  $\omega$  versus  $H_{a\perp}$ . In the case of parallel resonance the field ( $4\pi M_s - H_{k\perp}$ ) can be calculated from the slope of a plot of  $[(\omega/\gamma)^2 - H_{a\parallel}^2]$  versus  $H_{a\parallel}$ . Wherever possible the values of  $\gamma$  were obtained by measuring the slope of the  $\omega$  versus  $H_{a\perp}$  plot. Elsewhere the best values available from the literature were used (Tannenwald and Weber, 1961; Phillips, 1966).

The results of this investigation were consistent with the isotropic stress data referred to earlier except in the case of films thinner than 600 Å. This inconsistency made an independent stress determination desirable. Since films could be removed from the substrates without structural damage, it was possible to measure directly the isotropic strain  $\epsilon$  due to substrate constraint. With the assumptions that a film rigidly attached to a substrate is in a condition of constant isotropic strain in the plane and zero stress perpendicular, the isotropic stress was then calculated using the equation

$$\sigma = [\epsilon E / (1 - \nu)], \quad (1.4)$$

where  $E$  is Young's modulus and  $\nu$  is Poisson's ratio. An optical comparator with a resolution of  $2 \times 10^{-4}$  cm (corresponding to a strain of  $3 \times 10^{-4}$ ) was used to measure the diameter of the sample before and after relaxation of the isotropic strain, a reasonable average being obtained by measuring four film diameters  $45^\circ$  apart. Observed strains were an order of magnitude above the resolution of the comparator. Strain data were obtained for 51 Ni-49 Fe and pure Ni films as a function of thickness.

#### 1.4 Results and Discussion

##### 1.4.1 Comparison of Stress Dependent Perpendicular Anisotropy With Theory

Using the dispersion relations given in Eqs. (1.2) and (1.3), the effective perpendicular anisotropy fields with and without isotropic planar stress were obtained from the resonance data. The corresponding differences in perpendicular anisotropy energy  $\Delta K_{\perp}$  were calculated using bulk values of  $M_s$  (Bozorth, 1951). These differences are shown in Figs. 1-1 and 1-2 as a function of composition for the Ni-Fe and Ni-Co alloy systems, respectively. Only the predominantly fcc crystal structure regions of both Ni-Fe (Suzuki and Wilts, 1967) and Ni-Co (Suzuki, 1969) are included. In the bcc region of Ni-Fe and the mixture phase region of the Ni-Co alloys the observed values of  $\Delta K_{\perp}$  showed so much scatter that no comparison with theory was possible. As mentioned earlier, uncoated substrates were used as checks to insure uniformity between samples on coated and uncoated substrates. Except at pure Ni

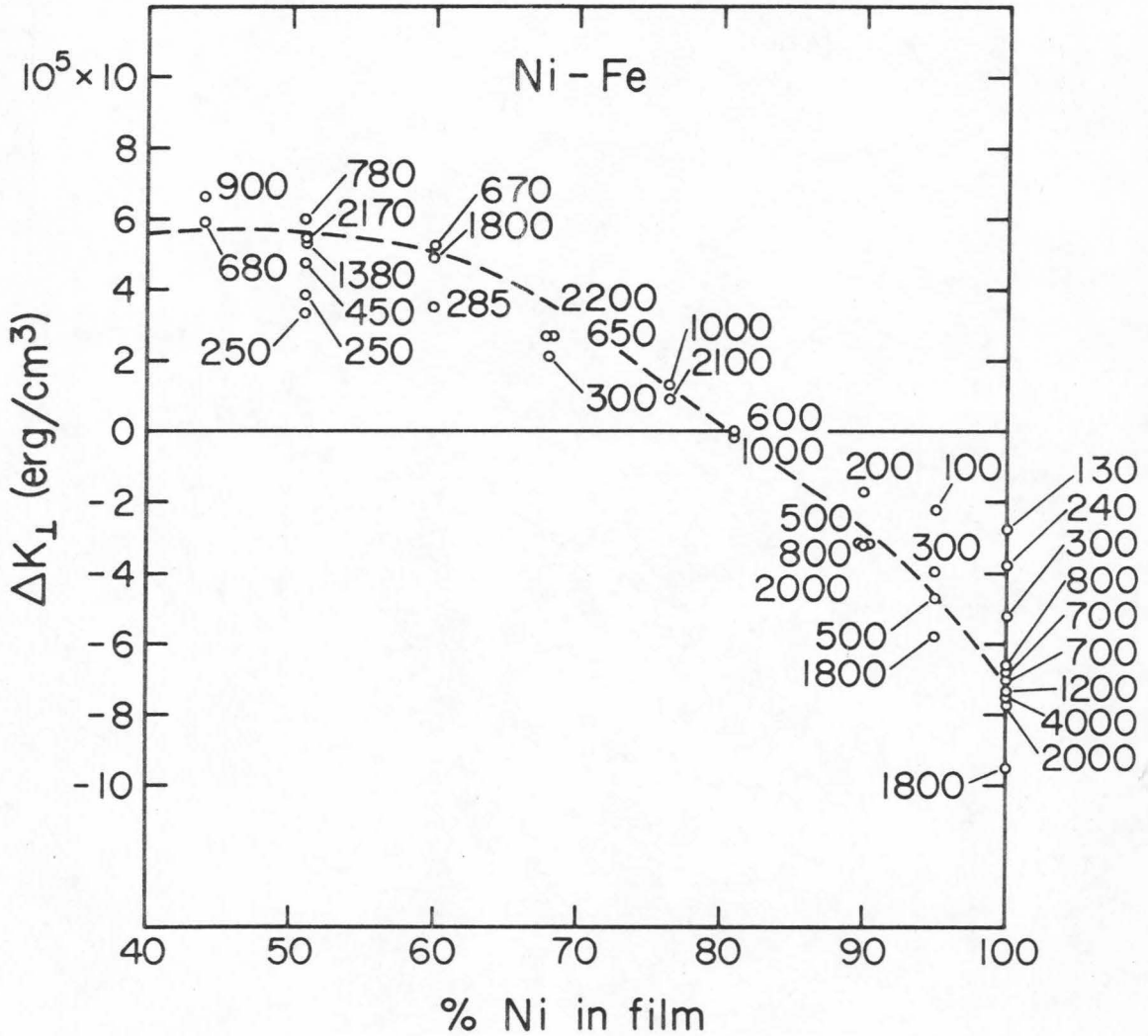


Fig. 1-1 Substrate constraint contribution to the perpendicular anisotropy in Ni-Fe alloys vs. weight percentage composition. Sample thicknesses are given in angstroms. The dashed line indicates the predicted value of  $\Delta K_{\perp}$  for an isotropic stress of  $1.4 \times 10^{10}$  dyn/cm<sup>2</sup>.

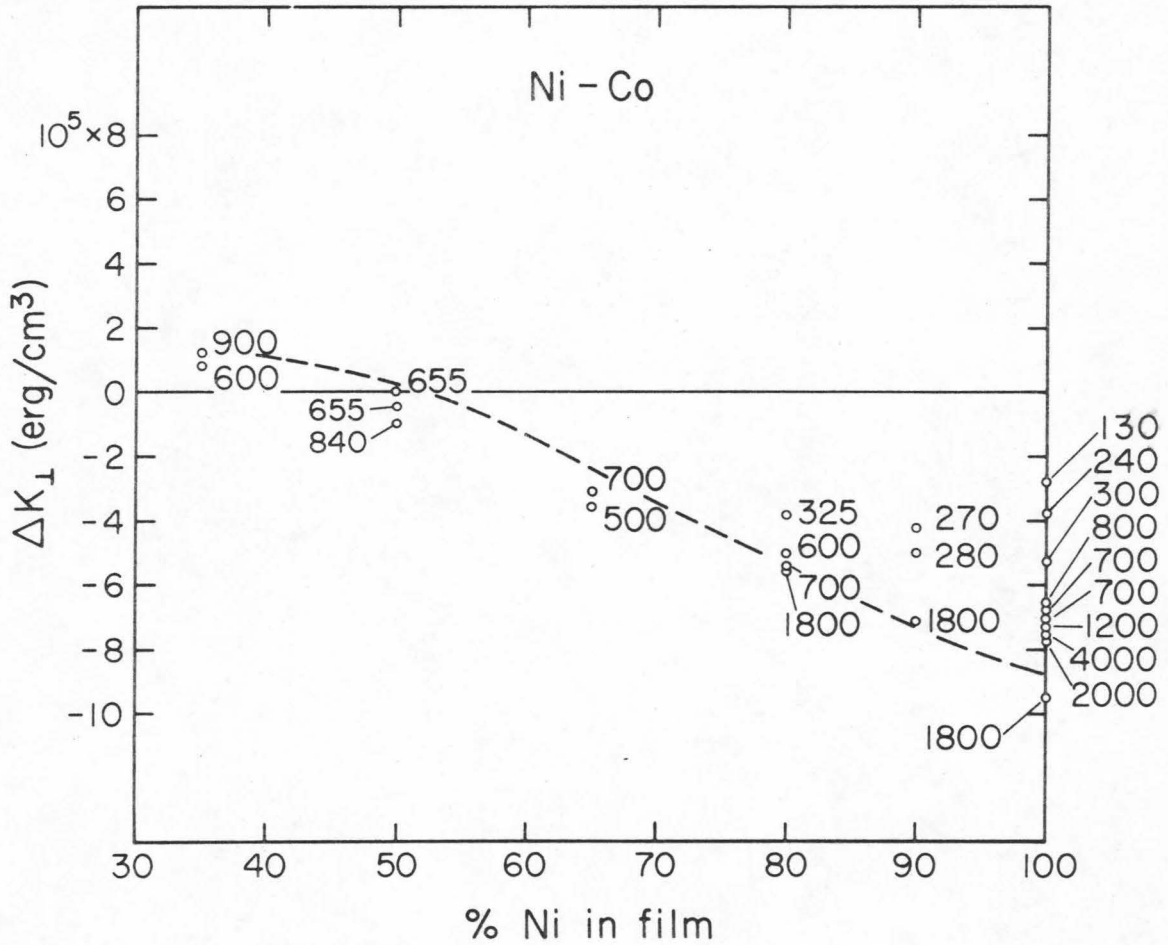


Fig. 1-2 Substrate constraint contribution to the perpendicular anisotropy in Ni-Co alloys vs. weight percentage composition. Sample thicknesses are given in angstroms. The dashed line indicates the predicted value of  $\Delta K_{\perp}$  for an isotropic stress of  $1.4 \times 10^{10} \text{ dyn/cm}^2$ .

the perpendicular anisotropy field with coated and uncoated substrates rarely differed by more than 100 Oe. For Ni films where  $\Delta H_{k_{\perp}}$  was as large as 4000 Oe, the maximum difference was 400 Oe.

From Figs. 1-1 and 1-2 it appears that  $\Delta K_{\perp}$  has a distinct thickness dependence. Films in both alloy systems, which are less than about 600 Å thick, exhibit a decrease in the magnitude of  $\Delta K_{\perp}$  with decreasing film thickness. For films thicker than 600 Å the measured value of  $\Delta K_{\perp}$  is essentially independent of thickness. This thickness dependence of  $\Delta K_{\perp}$  could be explained by the magnetostrictive model if the stress were also thickness dependent. In Figs. 1-3(a) and 1-4(a) the measured values of isotropic strain  $\epsilon$  for 100 Ni and 51 Ni-49 Fe films are shown as a function of thickness. Figures 1-3(b) and 1-4 (b) show the measured values of  $\Delta K_{\perp}$  as a function of thickness for 100 Ni and 51 Ni-49 Fe films. The observed thickness dependence of the strain is in disagreement with the data referenced earlier, but it correlates well with the observed thickness dependence of  $\Delta K_{\perp}$ . Where possible strain measurements were made on two films of equal thickness evaporated at the same time. For films evaporated simultaneously the strain values agreed within about 10% except for the 130 Å Ni samples which showed more scatter. Using Eq. (1.4) with the values  $2.07 \times 10^{12}$  dyn/cm<sup>2</sup> for Young's modulus of Ni and  $1.66 \times 10^{12}$  dyn/cm<sup>2</sup> for 51 Ni-49 Fe and a Poisson's ratio of 0.29 for both compositions (Marsh, 1938), the isotropic stress for films thicker than 600 Å is calculated to be about  $1.6 \times 10^{10}$  dyn/cm<sup>2</sup> for both compositions. Using values of  $\Delta K_{\perp}$  from Figs. 1-3(b) and 1-4(b) and values of the bulk magnetostriction constant for  $\lambda_s$  (Bozorth, 1951)

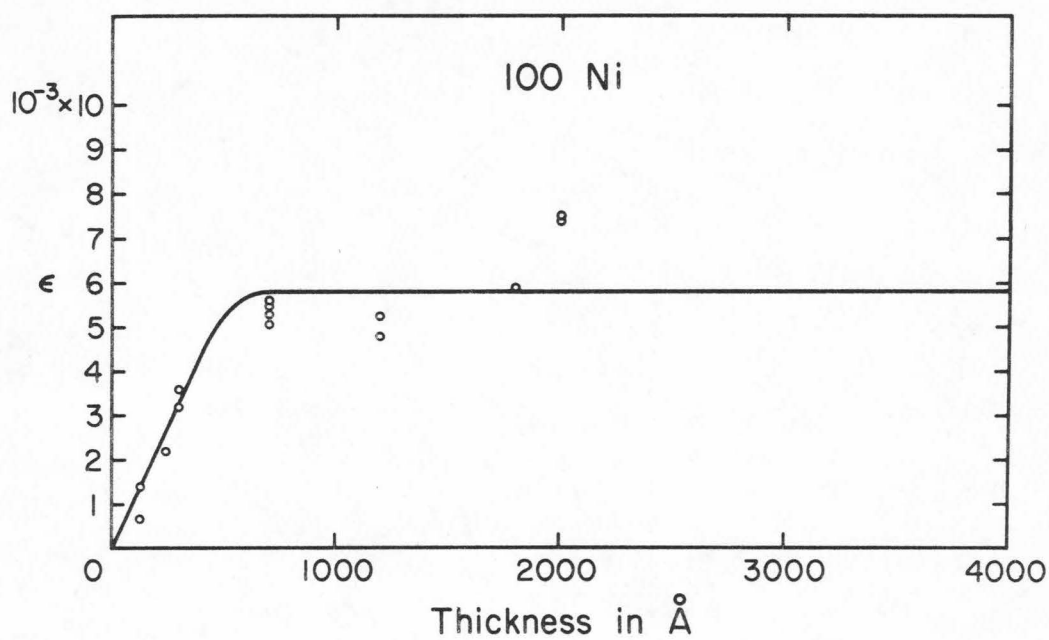


Fig. 1-3(a) Isotropic strain  $\epsilon$  vs. thickness for pure Ni films.

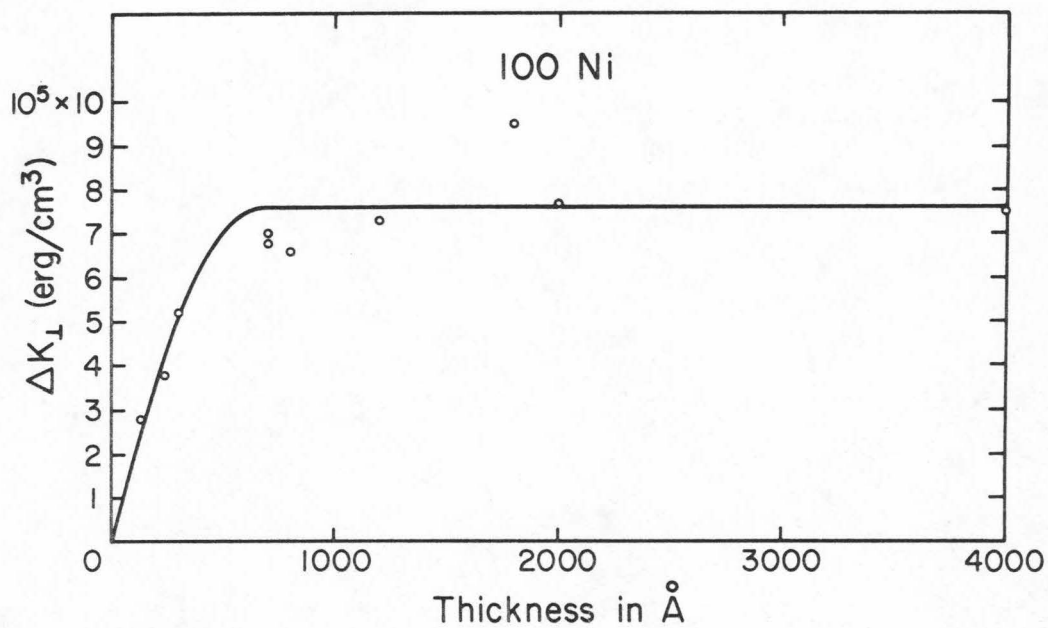


Fig. 1-3(b) Substrate constraint contribution to the perpendicular anisotropy  $\Delta K_{\perp}$  vs. thickness for pure Ni films.

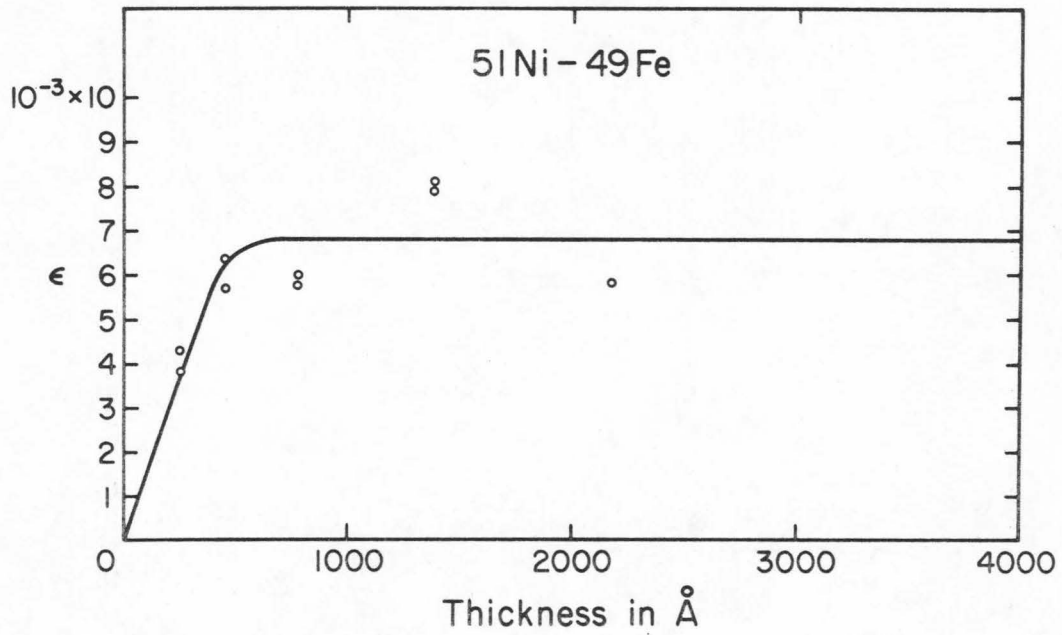


Fig. 1-4(a) Isotropic strain  $\epsilon$  vs. thickness for 51 Ni-49 Fe films.

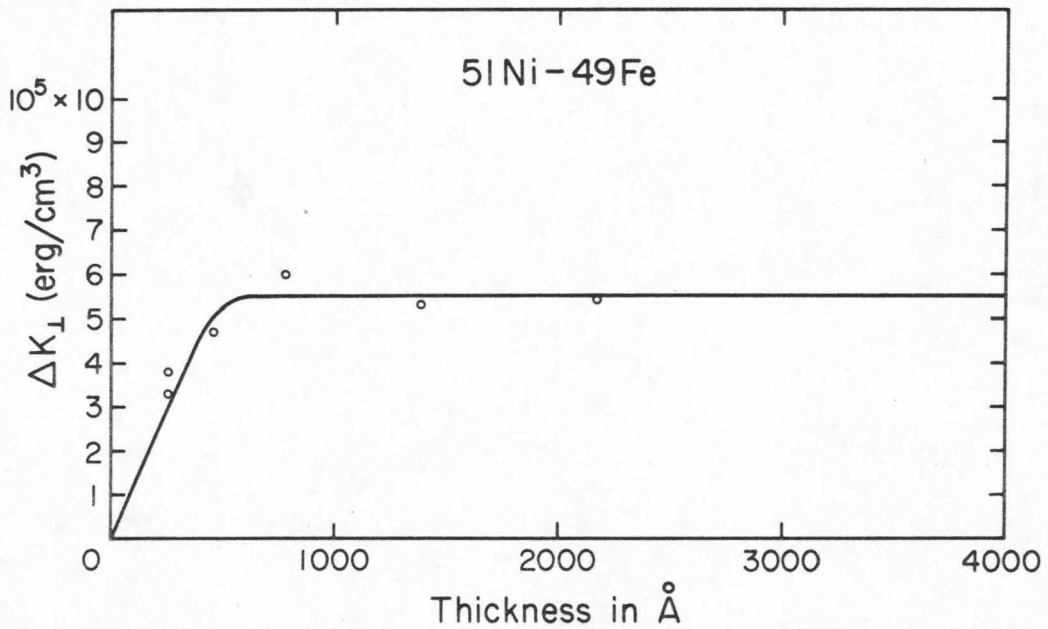


Fig. 1-4(b) Substrate constraint contribution to the perpendicular anisotropy  $\Delta K_{\perp}$  vs. thickness for 51 Ni-49 Fe films.

in Eq. (1.1), the stress in films thicker than  $600 \text{ \AA}$  is calculated to be about  $1.4 \times 10^{10} \text{ dyn/cm}^2$  for both compositions. Thus the thickness dependences of  $\epsilon$  and  $\Delta K_{\perp}$  are in agreement as to the shape of the dependence but differ about 15% in magnitude. Taking into account the uncertainty of  $E$ ,  $\lambda_s$ , and  $\nu$  for thin films, this is considered satisfactory agreement. The dashed lines in Figs. 1-1 and 1-2 show the values of  $\Delta K_{\perp}$  predicted by Eq. (1.1) using the bulk values of  $\lambda_s$  and a stress  $\sigma = 1.4 \times 10^{10} \text{ dyn/cm}^2$ . For all compositions the predicted values of  $\Delta K_{\perp}$  are in reasonable agreement with observed values for films thicker than  $600 \text{ \AA}$ .

The exchange term was omitted in the resonance conditions given by Eqs. (1.2) and (1.3). If the spins were strongly pinned at the film surface, the exchange term would be important, and the effective perpendicular anisotropy field as determined from these equations should be different in perpendicular resonance from that in parallel resonance particularly for the thinnest films. Experimentally the results of parallel and perpendicular resonance are essentially the same, showing that spin pinning is small and that the exchange correction for the first resonance mode is negligible. This is in agreement with the conclusions of Bajorek and Wilts (1971).

#### 1.4.2 Evidence for Another Source of Perpendicular Anisotropy

If the stress mechanism were the only source of the perpendicular anisotropy, then the films which have been removed from the substrates should exhibit no other perpendicular anisotropy than the shape anisotropy due to the sample geometry. The effective demagnetizing fields

measured by ferromagnetic resonance,  $4\pi M_{res}$ , are shown in Figs. 1-5 and 1-6 for Ni-Fe and Ni-Co films. All measurements are normalized to bulk saturation magnetization values given by Bozorth (1951). Data are given for samples as evaporated on the substrates and after removal from the substrates. In both alloy systems near 100 Ni there appears to be a significant perpendicular anisotropy present which cannot be explained by the macroscopic isotropic stress mechanism. Fujiwara and Sugita (1968) also observed an anomalous perpendicular anisotropy in Ni films stripped from the substrates. A possible explanation is that the vacuum is not good enough during the evaporation to yield bulk magnetization values in the films, but almost all previous work in this area is in agreement that a vacuum of  $10^{-6}$  Torr is sufficient to insure that the magnetization in films thicker than five hundred angstroms is within a few percent of values for bulk material. It is also difficult to see how a vacuum effect could depend on the composition of the samples. The same argument holds for any mechanism of preferential grain growth through the film thickness.

The possible presence of a microstress among the individual crystallites should also be considered. On the other hand such a source should be directly related to the magnetostriction constants which are zero at 81 Ni-19 Fe and near 50 Ni-50 Co, but the experimental results at these two compositions are not conclusive. At the 50 Ni-50 Co composition the apparent deviation of  $4\pi M_{res}$  from the bulk value of  $4\pi M_s$  may be within the experimental error, but at the 81 Ni-19 Fe composition the deviation of almost 10% from the bulk value is difficult to ignore. If the

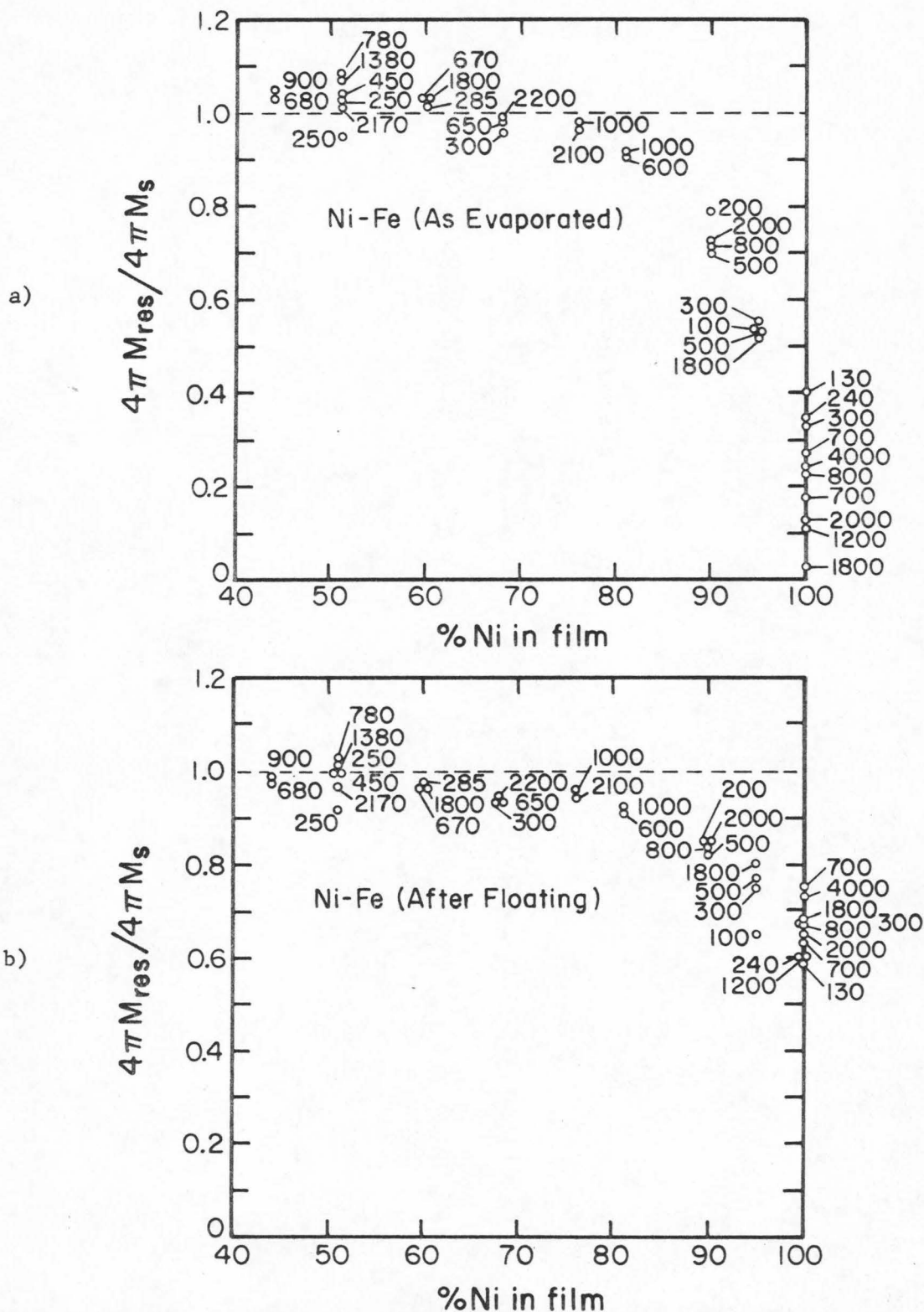


Fig. 1-5 Effective demagnetizing fields from resonance normalized to bulk  $4\pi M_s$ . Thicknesses are given in angstroms.

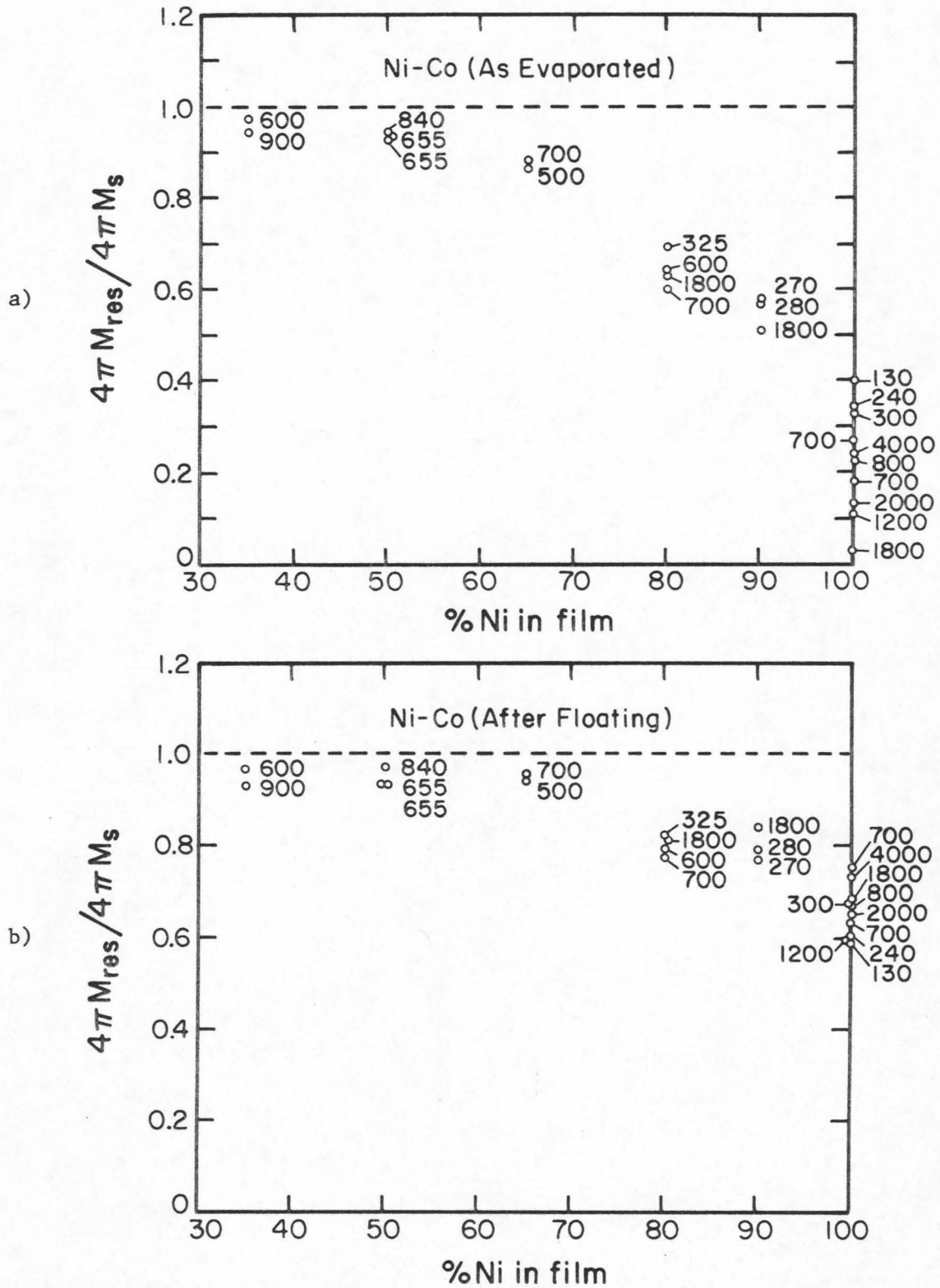


Fig. 1-6 Effective demagnetizing fields from resonance normalized to bulk  $4\pi M_s$ . Thicknesses are given in angstroms.

deviations from bulk values at 81 Ni-19 Fe and 50 Ni-50 Co are taken to be constant throughout the Ni-Fe and Ni-Co alloy compositions studied, the remaining perpendicular anisotropy shown in Figs. 1-5b and 1-6b appears qualitatively to be proportional to  $\lambda_s$ . This might be explainable by some model of stress among the crystallites. The stress among crystallites should change as a function of substrate temperature during evaporation, because it is known that the crystallite size increases with increasing substrate temperature. To study further a possible mechanism of intercrystalline stress, it should be instructive to measure the dependence of the anomalous perpendicular anisotropy on the substrate deposition temperature. Some other technique of removing the films from the substrate would have to be developed, since the water soluble material used in this study is useful only at temperatures below 150°C. At present no satisfactory explanation is available as to the source of this anomalous perpendicular anisotropy.

## Chapter 2

EFFECT OF SUBSTRATE CONSTRAINT ON THE  
CRYSTALLINE ANISOTROPY OF EPITAXIAL FILMS2.1 Introduction

In a single crystal the magnetocrystalline anisotropy energy density  $K_1$  is a measure of the dependence of the internal energy on the direction of magnetization in the sample. The magnetocrystalline anisotropy energy for cubic crystals can therefore be expressed in a polynomial series of the direction cosines  $(\alpha_1, \alpha_2, \alpha_3)$  of the internal magnetization with respect to the three cube edges. Only terms that exhibit the same symmetries as the crystal are nonzero. It can be shown quite simply that the first two terms of the energy can be expressed in the form

$$E_A = K_1(\alpha_1^2\alpha_2^2 + \alpha_2^2\alpha_3^2 + \alpha_1^2\alpha_3^2) + K_2\alpha_1^2\alpha_2^2\alpha_3^2 \quad (2.1)$$

where  $K_1$  and  $K_2$  are the lowest order anisotropy constants. If the magnetization is constrained to be in the (001) plane ( $\alpha_3 = 0$ ) of a cubic crystal, then the expression for the anisotropy energy becomes  $K_1\alpha_1^2\alpha_2^2$ , excluding terms of order higher than the sixth power.

The magnetization of a thin magnetic film which is grown epitaxially on a (001) plane of a single crystal substrate is constrained to be in this plane by the large demagnetizing field normal to the sample. As long as the film grows with the same crystalline orientation as the substrate, the only anisotropy constant of interest is  $K_1$ . Using this approach, several authors have measured  $K_1$  for thin films of Ni and

Ni-Fe alloys (Boyd, 1960; Chikazumi, 1961; Anderson, 1961; Freedman, 1962; Tsukahara and Kawakatsu, 1966; Brownlow, 1971). Most of this work was done with NaCl substrates, but Chikazumi used MgO as well and Brownlow used only MgO. Most of the measurements of  $K_1$  for samples grown on NaCl were made after the substrates had been dissolved and the sample transferred to a glass slide. Freedman, however, reported values of  $K_1$  for Ni films on NaCl and on glass after dissolving the NaCl.

The agreement among all these investigators is not very good. Boyd, Anderson, and Freedman report near bulk values (Bozorth, 1951) at pure Ni for films deposited on NaCl and subsequently transferred to glass. Chikazumi and Tsukahara and Kawakatsu report values about 50% higher than bulk for films treated by the same process. The reported values by Chikazumi and Brownlow for Ni films on MgO are about twice the bulk values. Brownlow, who did the most extensive survey of the Ni-Fe alloys, reports values which consistently differ from the bulk values as given by Bozorth. According to Bozorth,  $K_1$  is zero at 75% Ni while according to Brownlow the zero is at 63% Ni. In all these investigations the measurements have been made with the films constrained by substrates. Films removed from NaCl and put on glass no longer have the isotropic stress due to thermal mismatch of the substrate and film or to the deposition process, but the adherence of the film to the glass does not allow the sample to deform freely as the magnetization is rotated during a measurement of  $K_1$ . In order to make a better comparison with bulk values of  $K_1$ , it is necessary to measure the sample

in a condition of constant stress, presumably zero, rather than in a condition of constant strain as caused by adherence to a substrate.

The present investigation was undertaken to determine whether the anisotropy constants of freely floating epitaxial films were in better agreement with bulk values. Also it was possible to measure the difference between the anisotropy at constant strain and that at constant stress and to compare this difference with the theoretical prediction.

## 2.2 Theory

As discussed in the previous section, a film on a substrate is in a condition of constant strain. Therefore the elastic and magnetoelastic energy densities which depend on the strains can only contribute to the uniaxial anisotropy energy, not to the magnetocrystalline anisotropy (See Eqs. (2.2) and (2.3)). On the other hand a freely floating film can deform and has an additional contribution to the magnetocrystalline anisotropy energy density due to the presence of magnetostriction.

To calculate the anisotropy in this zero stress configuration it is necessary to find the equilibrium strains for an arbitrary direction of magnetization in the sample and then to use these strains in the expressions for the elastic and magnetoelastic energy densities. Terms with the same angular dependence as the magnetocrystalline anisotropy energy density given by Eq. (2.1) will contribute an additional anisotropy. The elastic energy density in a cubic crystal is

$$\begin{aligned}
E_{el} = & \frac{1}{2} C_{11} (e_{11}^2 + e_{22}^2 + e_{33}^2) \\
& + \frac{1}{2} C_{44} (e_{12}^2 + e_{23}^2 + e_{31}^2) \\
& + C_{12} (e_{11}e_{22} + e_{22}e_{33} + e_{33}e_{11}), \quad (2.2)
\end{aligned}$$

where  $C_{ij}$  are the elastic constants and  $e_{ij}$  are the strains. The magnetoelastic energy density to first order is written

$$\begin{aligned}
E_{mag-el} = & B_1 [e_{11}(\alpha_1^2 - \frac{1}{3}) + e_{22}(\alpha_2^2 - \frac{1}{3}) + e_{33}(\alpha_3^2 - \frac{1}{3})] \\
& + B_2 [e_{12}\alpha_1\alpha_2 + e_{23}\alpha_2\alpha_3 + e_{31}\alpha_3\alpha_1], \quad (2.3)
\end{aligned}$$

where the  $\alpha$ 's are the direction cosines of the magnetization relative to the cubic axes and the B's are the magnetoelastic coupling constants. For the stress free configuration the equilibrium strains are found by minimizing the total energy density

$$E = E_A + E_{el} + E_{mag-el}, \quad (2.4)$$

with respect to the  $e_{ij}$ . The results are given by the expressions

$$\begin{aligned}
e_{ii} &= \frac{-B_1}{C_{11} - C_{12}} (\alpha_i^2 - \frac{1}{3}) \\
e_{ij} &= \frac{-B_2}{C_{44}} \alpha_i \alpha_j \quad (i \neq j). \quad (2.5)
\end{aligned}$$

The magnetoelastic constants can be related to the magnetostriction constants by the relations

$$B_1 = -\frac{3}{2} (C_{11} - C_{12})\lambda_{100}$$

$$B_2 = -3C_{44}\lambda_{111} \quad . \quad (2.6)$$

The equations are simplified by assuming that the magnetization is constrained to be in the (001) plane such that  $\alpha_3$  is always zero. From the expression for  $E_A$  given in Eq. (2.1) it is clear that only terms with the angular dependence  $\alpha_1^2\alpha_2^2$  can contribute. This results, after collection of all the contributing terms in  $E_{el}$  and  $E_{mag-el}$ , in the additional anisotropy

$$\left[ \frac{9}{4} (C_{11} - C_{12})\lambda_{100}^2 - \frac{9}{2} C_{44}\lambda_{111}^2 \right] \alpha_1^2\alpha_2^2 \quad . \quad (2.7)$$

In summary the final results may be expressed by

$$K_1^{eff} |_{\text{constant strain}} = K_1$$

$$K_1^{eff} |_{\text{constant stress}} = K_1 + \left[ \frac{9}{4} (C_{11} - C_{12})\lambda_{100}^2 - \frac{9}{2} C_{44}\lambda_{111}^2 \right] \quad (2.8)$$

Now if  $\Delta K_1$  is defined as follows

$$\Delta K_1 \equiv K_1^{eff} |_{\text{constant strain}} - K_1^{eff} |_{\text{constant stress}} \quad (2.9)$$

then

$$\Delta K_1 = - \left[ \frac{9}{4} (C_{11} - C_{12})\lambda_{100}^2 - \frac{9}{2} C_{44}\lambda_{111}^2 \right] \quad . \quad (2.10)$$

This equation can be used to predict the change in effective magneto-crystalline anisotropy energy density between films constrained on a substrate and unconstrained films.

### 2.3 Experimental Methods

The vacuum system and the method of evaporation were the same as described in Sec. 1.3. The film thicknesses varied between 300 and 2000 Å. Four films were made simultaneously, one on a Corning 0211 glass slide, one on a polished MgO substrate, and two on polished MgO substrates coated with a thin evaporated layer of LiF. The MgO substrates were 1.2 cm square and 0.4 mm thick. They were cut so that the large surfaces corresponded to the (001) plane and the edges were parallel to the [100] or [110] direction. These substrates were purchased already cut and polished on one side to 1 $\mu$  particle size. Final polishing was done using 0.3 $\mu$  Al<sub>2</sub>O<sub>3</sub> particles with water on a silk polishing cloth, 0.05 $\mu$  Al<sub>2</sub>O<sub>3</sub> particles with water on velvet, and distilled water on velvet. An etch of one hour in triple distilled water at 40°C was then necessary to remove surface damage. The slides were rinsed in electronic grade acetone and placed in the vacuum system within a few minutes. Glass slides were cleaned only with electronic grade trichloroethylene and acetone. The substrates were then heated in the vacuum to 325°C by an external cartridge element heater with a temperature controller. The temperatures of the mask which held the substrates and the shutter which covered the mask were monitored by thermocouples so the substrate temperature was known to within a few degrees. When the temperature had stabilized (usually about a half hour), a 1000 Å layer of LiF was evaporated from powder placed on a tantalum boat onto two of the MgO substrates by partially opening the shutter. Within a few minutes the Ni or Ni-Fe films were evaporated onto all the substrates using an

induction heater. The substrate temperature was chosen to be 325°C to minimize any adverse effects to the LiF surface before the metallic film could be evaporated. Also Chikazumi (1961) and Brownlow (1971) found that 325°C was the minimum temperature at which complete epitaxy occurred on MgO. The plain MgO sample was used in order to check the consistency of the epitaxy of the films on the LiF coating. LiF was chosen rather than any of the other alkali halides because its lattice parameter of 4.03 Å was better matched to that of MgO (4.20 Å) and that of Ni-Fe (about 3.55 Å). NaCl and NaF were tried in the early stages of this investigation but both failed to give satisfactory results. Efforts to polish single crystal substrates of NaCl and NaF did not result in satisfactory surfaces.

The films on the LiF layer could not be floated off the MgO by simply placing it in water. Instead the sample had to be stripped from the substrate with brown paper tape which had water soluble glue. The tape was moistened with water and then was pressed firmly onto the film and substrate. After being allowed to dry for about five minutes, the tape with the film attached was carefully peeled from the substrate. The film was then removed by placing the tape in water and was subsequently transferred to a glass slide. Before the film dried on the substrate, glycerin was substituted for the water so that the film would remain freely floating for hysteresis loop tracer measurements and torquemeter measurements (Humphrey and Johnston, 1962). After the films were measured in an unconstrained condition, the samples were refloated on water, picked up on another clean glass slide, and allowed to settle

down on the new substrate. Once the water had completely evaporated the film adhered firmly to the substrate. In this constrained condition the films were measured again.

#### 2.4 Results and Discussion

The predicted values of  $\Delta K_1$  from Eq. (2.10) are shown in Fig. 2-1 for disordered and ordered Ni-Fe alloys assuming bulk elastic constants (Einspruch and Claiborne, 1964) and bulk magnetostriction constants (Bozorth and Walker, 1953). The experimental values are shown for comparison with the predicted values. The agreement is reasonable for films ranging in composition from 50% to 90% Ni. At pure Ni there appears to be a large deviation, but it must be remembered that the observed  $\Delta K_1$  still represents only about 20% of the total magnetocrystalline anisotropy for Ni samples. Nevertheless the discrepancy is believed to be real. Changes in  $\Delta K_1$  due to ordering effects are predicted to be very small, so they will be ignored at this time. It has been assumed that the elastic constants of ordered and disordered bulk material are the same, since measurements of Young's modulus in ordered and disordered bulk samples show that the changes are at most only a few percent (Köster, 1943).

In Fig. 2-2 the experimental values of  $K_1$  for unconstrained thin films are compared with bulk data for quenched samples (Bozorth and Walker, 1953). At pure Ni the thin film value is still too large in magnitude. Agreement is good from about 60% to 90% Ni but there is a significant deviation at the 50% Ni composition. It is interesting to note that a value of  $+ 33 \times 10^3 \text{ erg/cm}^3$  has been reported for  $K_1$  of bulk

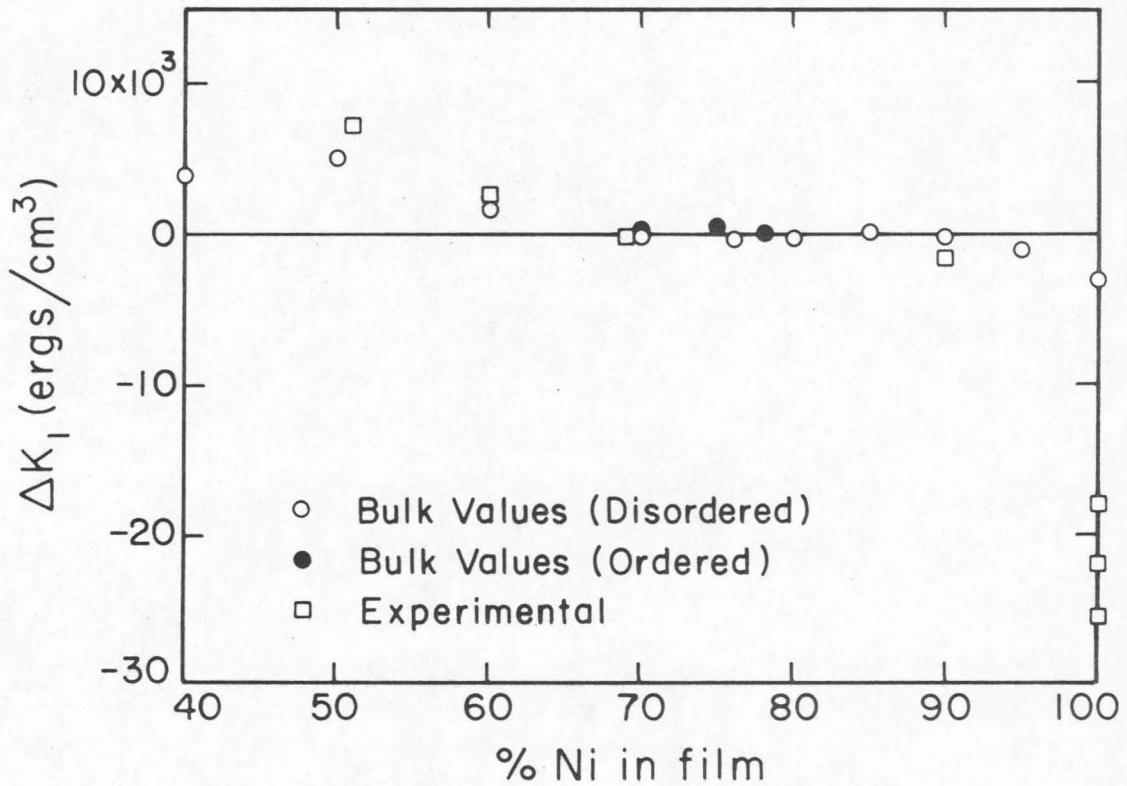


Fig. 2-1 Measured differences between  $K_1$  of constrained and unconstrained Ni-Fe films vs. weight percentage composition. Predicted changes (Eq. 2.10) based on ordered and disordered bulk data are also shown.

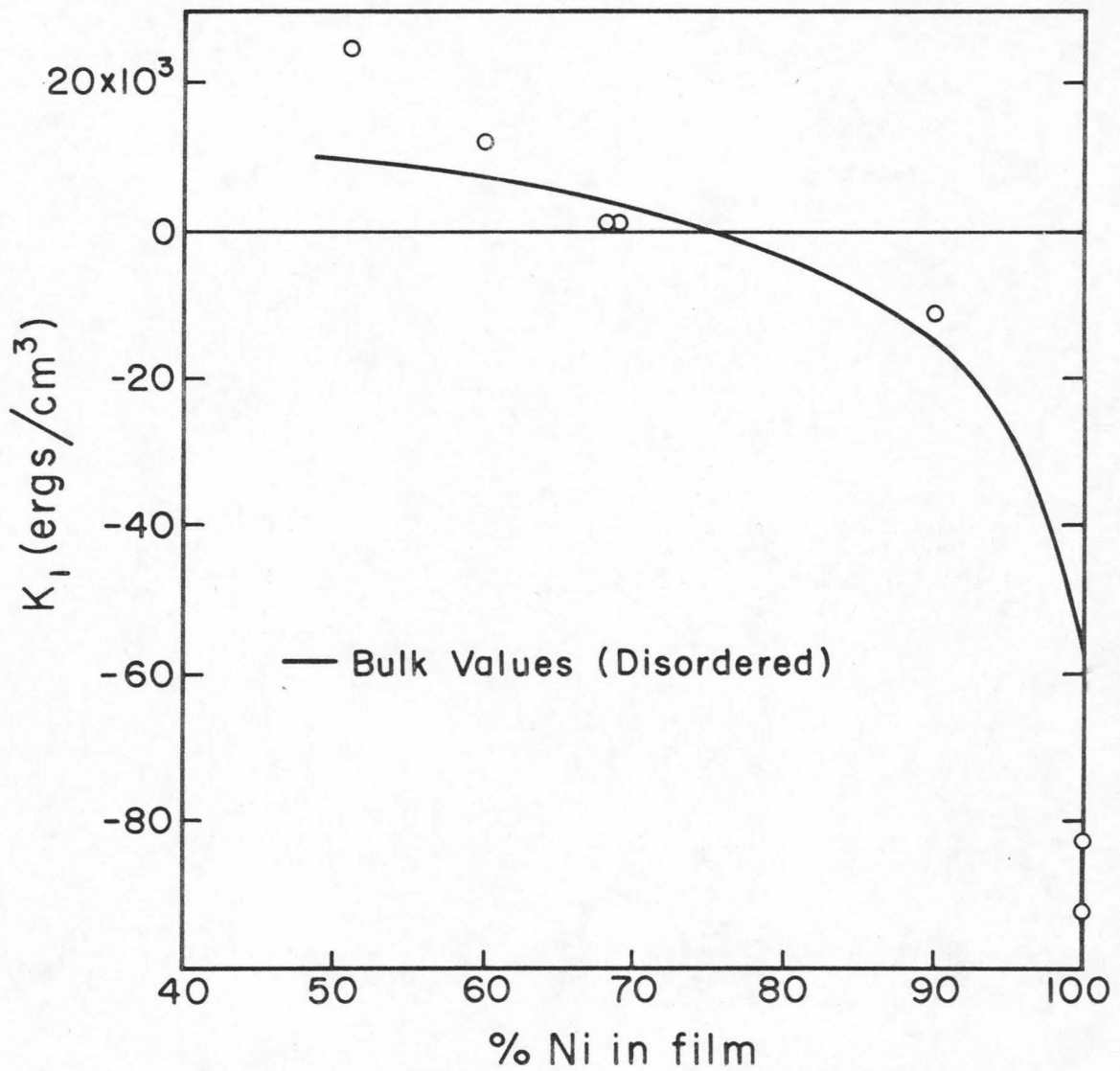


Fig. 2-2 Measured values of  $K_1$  for unconstrained Ni-Fe films vs. weight percentage composition. The solid line indicates measured values of disordered bulk samples.

material at 50 Ni-50 Fe (Kleis, 1936). This value is in much better agreement with the present data but is almost certainly less reliable than the value of Bozorth and Walker.

At some compositions, measurements of  $K_1$  for films attached to the substrate before removal differed significantly from those measurements made after the removal process and the film again was constrained by a substrate. The effect was most prominent at the 51% Ni point where the value of  $K_1$  after the removal process was about  $10 \times 10^3$  erg/cm<sup>3</sup> larger than the original value. At 68% Ni this difference was about  $1 \times 10^3$  erg/cm<sup>3</sup> and at 90% Ni about  $6 \times 10^3$  erg/cm<sup>3</sup>. The difference at Ni was small compared to the value of  $K_1$  and therefore difficult to measure, but is approximately  $5 \times 10^3$  erg/cm<sup>3</sup>. Table 2.1 gives values of  $K_1$  for thin films under different conditions of measurement as compared to bulk values. Unconstrained values are for films floating on glycerin. Films constrained after removal are those which have been removed from the MgO substrate, floated, and allowed to dry on glass slides. The constrained as evaporated values are for films still on the MgO substrates with the LiF intermediate layer.

The value of  $K_1$  measured for unconstrained Ni films is in better agreement with bulk values for almost all compositions, but the discrepancy persists. Also the value of  $\Delta K_1$  at pure Ni gives poor agreement with bulk predictions. It may be necessary to include higher order magnetostriction constants in the expression for  $\Delta K_1$  (Mason, 1951), but no reliable experimental data exist for the higher order constants. Freedman (1962) proposed that the high  $K_1$  values for films on NaCl were

TABLE 2.1

<u>Composition</u>	<u>Bulk Value</u> <sup>*</sup>	<u>Unconstrained Film</u>	(K <sub>1</sub> )	
			<u>Constrained Film After Removal</u>	<u>Constrained Film As Evaporated</u>
100 Ni	- 59	- 82	- 100	- 96
90 Ni	- 16	- 10.9	- 12.5	- 18.3
68 Ni	+ 3	+ 1.6	+ 1.5	+ 0.9
60 Ni	+ 7	+ 12.3	+ 14.7	+ 8.5
51 Ni	+ 10	+ 25	+ 32	+ 22

\* According to quenched values of Bozorth and Walker (1953).

Units are 10<sup>3</sup> ergs/cm<sup>3</sup>

caused by isotropic stress in the sample due to thermal mismatch of film and substrate. This stress affected  $K_1$  through the higher order magnetostriction constants. The thermal mismatch between Ni and MgO is very small so that contributions to  $K_1$  by this mechanism should be small. Experimentally the values of  $K_1$  for films on MgO are even larger in magnitude than those reported for films on NaCl. In order to answer some of the questions raised here, it will be necessary to know what strain exists in an epitaxial film on a single crystal substrate. Possibly a technique similar to that described in Chapter 1 would be appropriate, but it is a difficult problem.

## Chapter 3

FORMATION OF ORDERED  $\text{Ni}_3\text{Fe}$  AND ITS EFFECTS  
ON THE PROPERTIES OF Ni-Fe THIN FILMS3.1 Introduction

The  $\text{Ni}_3\text{Fe}$ <sup>\*</sup> structure corresponds to an fcc lattice with Fe atoms at the corners of the cubes and Ni atoms at the centers of the cube faces. In a perfectly ordered crystal all Fe atoms have 12 Ni nearest neighbors, and all Ni atoms have 4 Fe and 8 Ni nearest neighbors. This complete uniformity of structure is the basis for the term long-range order. In a disordered state the atomic nearest neighbors for a given atom can only be known in terms of probabilities. Since the local environment of the atoms changes significantly from disorder to order, it is reasonable to expect changes in the magnetic properties of a material which are so dependent on the exchange interaction which in turn changes with local environment.

Leech and Sykes (1939) were the first to observe superlattice lines in  $\text{Ni}_3\text{Fe}$  with X-ray diffraction. Other workers have studied the magnetic properties of Ni-Fe alloys around the atomic composition  $\text{Ni}_3\text{Fe}$  (Grabbe, 1940; Wakelin and Yates, 1953; Bozorth and Walker, 1953; Taoka and Ohtsuka, 1954). Shull and Wilkinson (1955) observed superlattice reflections with neutron diffraction for  $\text{Ni}_3\text{Fe}$ . These studies were all carried out using samples prepared from bulk specimens. Up to the present time no comprehensive study of ordering in evaporated thin films

---

\*This corresponds to a weight percentage composition of 75.9 Ni-24.1 Fe.

of Ni-Fe has been found in the literature. Boyd (1960) annealed thin epitaxial films with compositions in the neighborhood of  $\text{Ni}_3\text{Fe}$  both in vacuum and in forming gas in an attempt to induce ordering. Significant changes in  $K_1$  reportedly occurred only at 81 Ni-19 Fe. The sample structure was observed by electron diffraction after being annealed, but no noticeable changes in the structure were seen except the loss of stacking faults. The present study was then undertaken to discover whether ordered  $\text{Ni}_3\text{Fe}$  could be produced in thin films, and if so to see how this affected the magnetic properties. The effects on saturation magnetization, magnetocrystalline anisotropy  $K_1$ , and the magnetostriction constants have been studied.

### 3.2 Experimental Methods and Theoretical Predictions

Samples were prepared by vapor deposition using the system described in Chap. 1. For polycrystalline films, glass substrates were used as described earlier. For epitaxial films, MgO substrates were polished as described in Sec. (2.2). The substrates were held at  $325^\circ\text{C}$  during the evaporation. Samples ranged in thickness from 250-4000 Å. The films were removed from the vacuum system so that all pertinent measurements could be made. The samples were then annealed in the same vacuum system at pressures well below  $10^{-7}$  Torr. Based on measurements of magnetocrystalline anisotropy  $K_1$ , the highest degree of order was obtained when the annealing temperature was maintained between 400 and  $410^\circ\text{C}$ . Samples for electron diffraction were evaporated on an intermediate layer of LiF as described in the previous chapter. Magnetization measurements were made on a low frequency ( $\sim 10$  Hz) hysteresis

loop tracer, so changes in magnetization could be measured quite easily on the thicker films. The magnetocrystalline anisotropy  $K_1$  was measured with a high field torquemeter. The weight percentage film compositions were determined by X-ray fluorescence.

Strain sensitivity measurements, that is the change in uniaxial anisotropy field for a given uniaxial strain, were measured by ferromagnetic resonance. A special stripline, which was equipped to bend the substrate around two points (Brownlow, 1971), was used to apply the uniform uniaxial strain. The substrates were cut so that the edges were in a [100] or [110] direction. It can be shown (see Appendix 1) that the application of a uniform strain  $e$  along the [100] direction in the (001) plane results in a uniaxial anisotropy given by

$$E_{K_{100}} = \frac{3}{2} (C_{11} - C_{12}) \lambda_{100} e \sin^2 \phi = K_{100} \sin^2 \phi, \quad (3.1)$$

where the C's are the elastic constants,  $\lambda_{100}$  is the saturation magnetostriction in the [100] direction, and  $\phi$  is the angle between the magnetization and the applied strain. For a uniform strain along the [110] direction in the (001) plane the induced uniaxial anisotropy is given by

$$E_{K_{110}} = 3 C_{44} \lambda_{111} e \sin^2 \phi = K_{110} \sin^2 \phi, \quad (3.2)$$

where  $\lambda_{111}$  is the saturation magnetostriction in the [111] direction.

The dispersion relation for parallel ferromagnetic resonance (dc magnetic field in the film plane) is given by Bozorth (1951) for the case of a thin cubic crystal cut parallel to the (001) plane as

$$\begin{aligned}
\left(\frac{\omega}{\gamma}\right)^2 = & \{H_{a\parallel} + 4\pi M_s + \frac{K_1}{2M_s} (3 + \cos 4\phi) \\
& + \frac{K_2}{4M_s} (1 - \cos 4\phi) + \frac{K_u}{M_s} [1 + \cos 2(\phi - \psi)]\} \\
& \times \{H_{a\parallel} + \frac{2K_1}{M_s} \cos 4\phi + \frac{2K_u}{M_s} \cos 2(\phi - \psi)\} \quad (3.3)
\end{aligned}$$

Here  $\omega$  is the resonant frequency,  $\gamma$  the gyromagnetic ratio,  $H_{a\parallel}$  the applied dc field in the film plane,  $M_s$  the saturation magnetization, and  $K_u$  the uniaxial anisotropy. The first and second order crystalline anisotropy constants are given by  $K_1$  and  $K_2$ . The angles  $\phi$  and  $\psi$  are the angles between the magnetization and the [100] crystallographic direction and between the easy axis of the uniaxial anisotropy  $K_u$  and the [100] direction, respectively. In the case where the magnetization is in the [010] direction and the strain is in the [100] direction, Eq. (3.3) reduces to

$$\left(\frac{\omega}{\gamma}\right)^2 = [H_{a\parallel} + 4\pi M_s + \frac{2K_1}{M_s}] \times [H_{a\parallel} + \frac{2K_1}{M_s} - \frac{2K_u}{M_s}] \quad (3.4)$$

and likewise for the magnetization in the  $[1\bar{1}0]$  direction and the strain in the [110] direction, the equation gives

$$\left(\frac{\omega}{\gamma}\right)^2 = [H_{a\parallel} + 4\pi M_s + \frac{K_1}{M_s} + \frac{K_2}{2M_s}] \times [H_{a\parallel} - \frac{2K_1}{M_s} - \frac{2K_u}{M_s}] \quad (3.5)$$

For the Ni-Fe alloys of interest here  $|4\pi M_s| \gg |\frac{2K_1}{M_s}|$  or  $|\frac{K_2}{2M_s}|$ . The uniaxial anisotropy  $|\frac{2K_u}{M_s}| \ll |4\pi M_s|$  and for the frequencies used in the experiment the applied field  $H_{a\parallel} \ll 4\pi M_s$ . Thus for resonance at a fixed frequency  $\omega$ , the shift in the applied field necessary for resonance when a uniform uniaxial strain is applied is very nearly

equal to the anisotropy field  $\Delta H_k = \frac{2\Delta K_u}{M_s}$  induced by the strain. Data were taken of  $\Delta H_k$  as a function of the strain  $e$ . The strain sensitivity  $\frac{\Delta H_k}{e}$  was then calculated from the slope of this graph. The calibration of the applied strain was accomplished by the use of strain gages.

Expressions for the strain sensitivities in the [100] and [110] directions are obtained from Eqs. 3.1 and 3.2. It follows that

$$\frac{\Delta H_{k100}}{e} = \frac{3(C_{11} - C_{12})\lambda_{100}}{M_s}, \quad (3.6)$$

and

$$\frac{\Delta H_{k110}}{e} = \frac{6 C_{44} \lambda_{111}}{M_s}, \quad (3.7)$$

for the [100] and [110] directions, respectively.

For polycrystalline films on glass substrates the predictions of two models are compared with the experimental results. The assumptions that the applied strain is uniform through the film thickness and that the magnetization is constrained to lie in the film plane by the shape demagnetizing field are made for both models.

The first model to be discussed is the isotropic material model. This assumes that a polycrystalline film with randomly oriented crystallites can best be approximated by a film of isotropic material. In a bulk sample of isotropic material the uniaxial anisotropy due to a uniform uniaxial stress  $\sigma$  applied at an angle  $\phi$  with respect to the magnetization is predicted to be

$$E_{K_\sigma} = \frac{3}{2} \lambda_s \sigma \sin^2 \phi \quad , \quad (3.8)$$

where  $\lambda_s$  is the saturation magnetostriction constant (Bozorth, 1951). The condition of a thin film on a thin substrate when the substrate is bent uniformly is a uniform uniaxial strain in the film plane and zero stress perpendicular to the plane. It can be shown (see Appendix 2) that the anisotropy induced in the thin film by the uniform strain  $e$  is

$$E_{K_e} = \frac{3}{2} \frac{E\lambda_s}{1+\nu} e \sin^2 \phi = K_e \sin^2 \phi \quad , \quad (3.9)$$

where  $E$  is Young's modulus,  $\nu$  is Poisson's ratio, and  $\phi$  is now the angle between the applied strain and the magnetization. The strain sensitivity is given by

$$\frac{\Delta H_{k_e}}{e} = \frac{3E\lambda_s}{(1+\nu)M_s} \quad . \quad (3.10)$$

This change in uniaxial anisotropy may be measured by ferromagnetic resonance techniques as described previously. The only modification to Eq. (3.3) is the deletion of the terms involving  $K_1$  and  $K_2$ , the crystal-line anisotropy constants.

The second model is based on the assumption that the film is made up of individual crystallites but that these crystallites are constrained by the substrate and have no interaction with each other. Using this model, Brownlow (1971) and Brownlow and Wilts (1971) derived an expression for the uniaxial anisotropy induced in a polycrystalline film by a uniform strain. Their result is obtained by taking an

average of the expression for the induced anisotropy in a single cubic crystal due to a uniform strain (Eq. (A-1.5) in Appendix 1). The average is taken over all possible directions of the saturation magnetization and applied strain relative to the cubic axes of a single crystallite under the constraint that the angle  $\phi$  between the strain and magnetization is constant. The prediction for the strain induced uniaxial anisotropy is given by

$$E_{K_{\text{poly}}} = \frac{3}{10} e \{2(C_{11} - C_{12})\lambda_{100} + 6 C_{44}\lambda_{111}\} \sin^2 \phi . \quad (3.11)$$

The corresponding strain sensitivity is

$$\frac{\Delta H_{k_{\text{poly}}}}{e} = \frac{6}{5M_s} [(C_{11} - C_{12})\lambda_{100} + 3 C_{44}\lambda_{111}]. \quad (3.12)$$

### 3.3 Confirmation of Ni<sub>3</sub>Fe Structure

In order to confirm the existence of Ni<sub>3</sub>Fe in the annealed samples, it was necessary to use some technique to observe the crystal structure. X-ray diffraction was avoided because the low counting rates from thin films would make it a very difficult measurement. On the other hand transmission electron diffraction is well suited for thin films. Since films evaporated on the LiF intermediate layer could be removed from the substrates, samples for use in transmission electron diffraction could be obtained even after annealing by picking up small pieces of the film on fine mesh Cu-grids. The electron diffraction pictures were taken with the electron beam normal to the (001) plane of the thin film sample. Using an RCA EMU 3E electron microscope at 100 kV, the superlattice spots are clearly visible as shown in Fig. 3-1. The

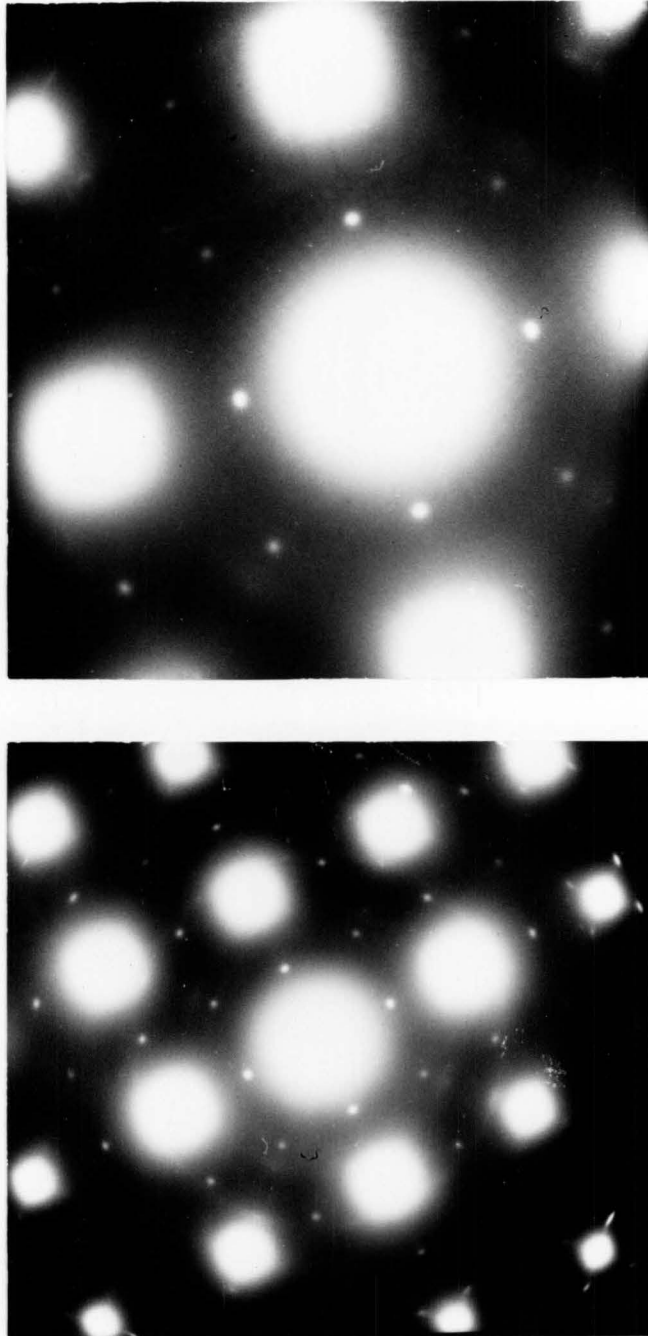


Fig. 3-1 Electron diffraction photographs of a 77 Ni-23 Fe sample after annealing.

sample had been annealed for 360 hours. The presence of the (100) and (110) reflections confirms the existence of the ordered  $\text{Ni}_3\text{Fe}$  structure since these reflections are forbidden in disordered fcc materials. The (001) and (002) atomic planes are indistinguishable in a disordered material, but in the ordered crystal lattice these two planes are no longer identical, the (001) plane containing half Ni and half Fe atoms and the (002) plane containing all Ni atoms. The intensity of the superlattice spots depends on the relative electron scattering amplitudes of Ni and Fe. For elements with highly different electronic structures and atomic sizes the difference in scattering amplitudes is significant, but this is not the case for Ni and Fe, therefore the superlattice spots are faint. The nearly equal X-ray scattering amplitudes of Ni and Fe made it difficult to confirm the existence of  $\text{Ni}_3\text{Fe}$  in bulk materials by X-ray diffraction. Several years elapsed after the  $\text{Ni}_3\text{Fe}$  structure was proposed as an explanation for resistivity measurements before the successful confirmation of this structure by X-ray diffraction (Leech and Sykes, 1939).

### 3.4 Results

#### 3.4.1 Effect of Ordering on Saturation Magnetization

The saturation magnetizations of films both on glass and MgO substrates have been measured by means of a hysteresis loop tracer before and after annealing to produce order. In Fig. 3-2 the data are shown for representative samples near the  $\text{Ni}_3\text{Fe}$  composition. The effect on  $4\pi M_s$  is largest at  $\text{Ni}_3\text{Fe}$ , but it is apparent over quite a broad composition range. The solid line in the figure is based on data by

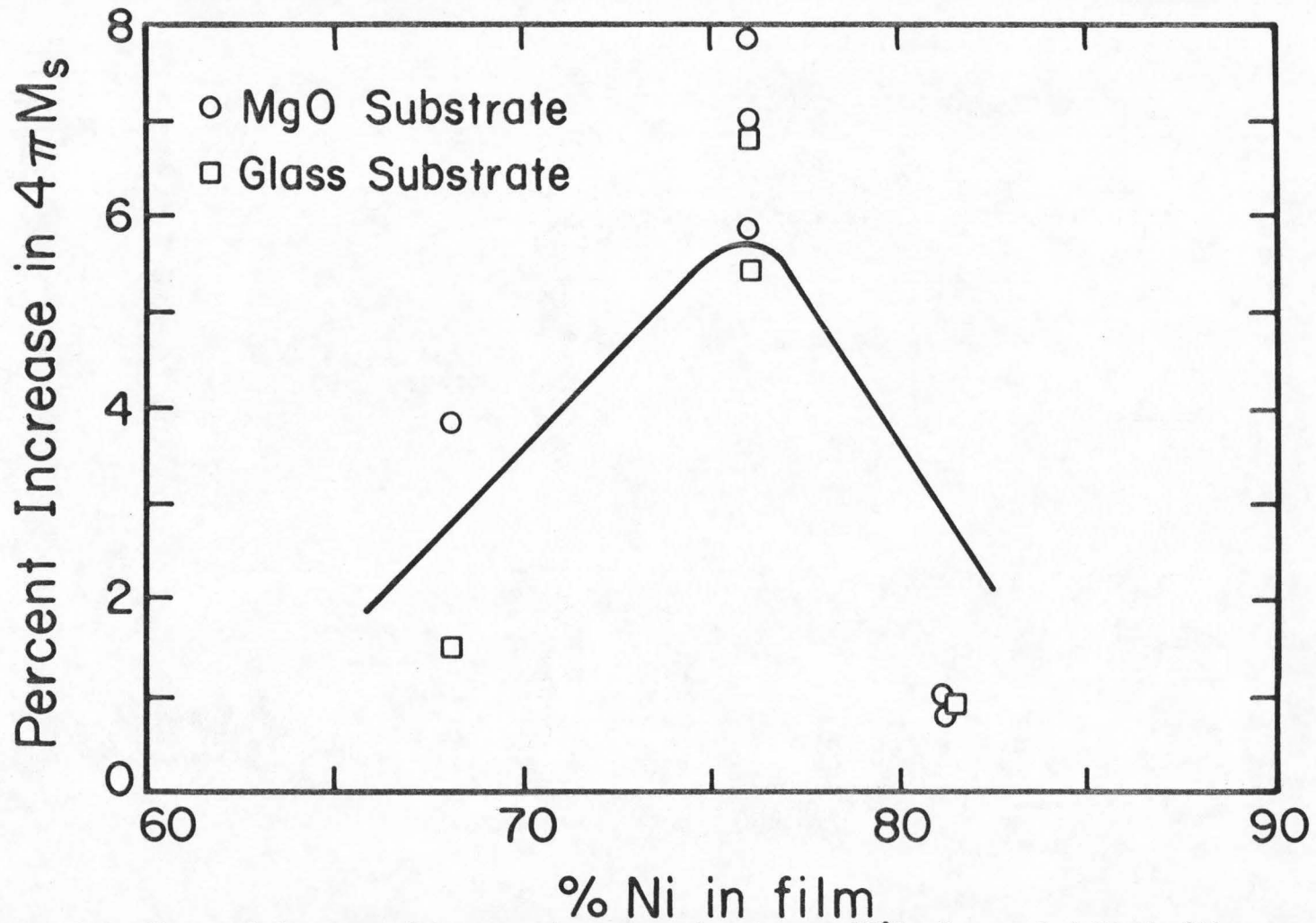


Fig. 3-2 Observed increase in saturation magnetization at 25°C of annealed Ni-Fe films vs. weight percentage composition. The solid line shows bulk data by Grabbe (1940).

Grabbe (1940), who made measurements on bulk samples before and after annealing. The thin films data for both epitaxial and polycrystalline films are in reasonably good agreement with the bulk data.

#### 3.4.2 Effect of Ordering on $K_1$

In order to make a direct comparison between the crystalline anisotropy  $K_1$  of thin films and  $K_1$  of bulk materials, the films should ideally be measured in an unconstrained condition as discussed in Chap. 2. After being annealed for long periods of time, the films could not be removed from the substrates with the LiF intermediate layer without being badly damaged. This made measurements of  $K_1$  on unconstrained samples impossible, thus all measurements were made on films constrained on MgO substrates. Since ordering occurs in compositions near  $Ni_3Fe$ , it is only necessary to consider the effect of constraint for compositions in this region.

Table 2.1 indicates that the difference between  $K_1$  measured for films as evaporated on MgO and for unconstrained films is very small at 68 Ni-32 Fe which is close to  $Ni_3Fe$ . At 60 Ni-40 Fe and 90 Ni-10 Fe the differences in  $K_1$  for the two measurements are significantly larger, but these compositions are far enough away from  $Ni_3Fe$  so that the final conclusions about the effect of ordering on  $K_1$  should not be changed because of the measurements on constrained samples. This argument would be invalid, if experimentally annealing produced large changes in  $K_1$  at compositions far from  $Ni_3Fe$ . It has been found that this is not the case; therefore, the experimental results would be modified only slightly by measuring the  $K_1$  of unconstrained films. It is also assumed

that the elastic constants of ordered and disordered samples are unchanged. This has been verified in bulk polycrystalline samples by measurements of Young's modulus  $E$  before and after annealing (Köster, 1943). Changes of only 2-3% were observed.

The values of  $K_1$  for annealed and unannealed films on MgO are shown in Fig. 3-3. Except for the samples at 62 Ni and 88 Ni, all the samples were annealed at least 350 hours between 400° and 410°C in vacuum. The films were taken out of the vacuum system every few days to check the progress of the ordering by measurements of  $K_1$ . When  $K_1$  stopped changing significantly with further annealing, it was assumed that the degree of order was as complete as could be obtained by this method. The final measurements of  $K_1$  after the last anneal are shown in the figure. The sample at 88 Ni was only annealed 150 hours before changes in  $K_1$  were small. At 62 Ni changes in  $K_1$  were small after 275 hours of annealing.

In Fig. 3-4 the values of  $K_1$  as a function of annealing time are shown for three representative samples. For annealing times longer than 350 hours the values of  $K_1$  continue to change only 10% or less. This was considered to be small so that 350 hours was taken to be adequate time to produce almost complete ordering in compositions between 68 Ni and 81 Ni. Outside this composition range shorter annealing times seemed to be adequate.

The solid and dashed lines in Fig. 3-3 are the measurements of  $K_1$  in disordered and ordered bulk single crystals according to Bozorth and Walker (1953). The agreement between the thin film values and the bulk

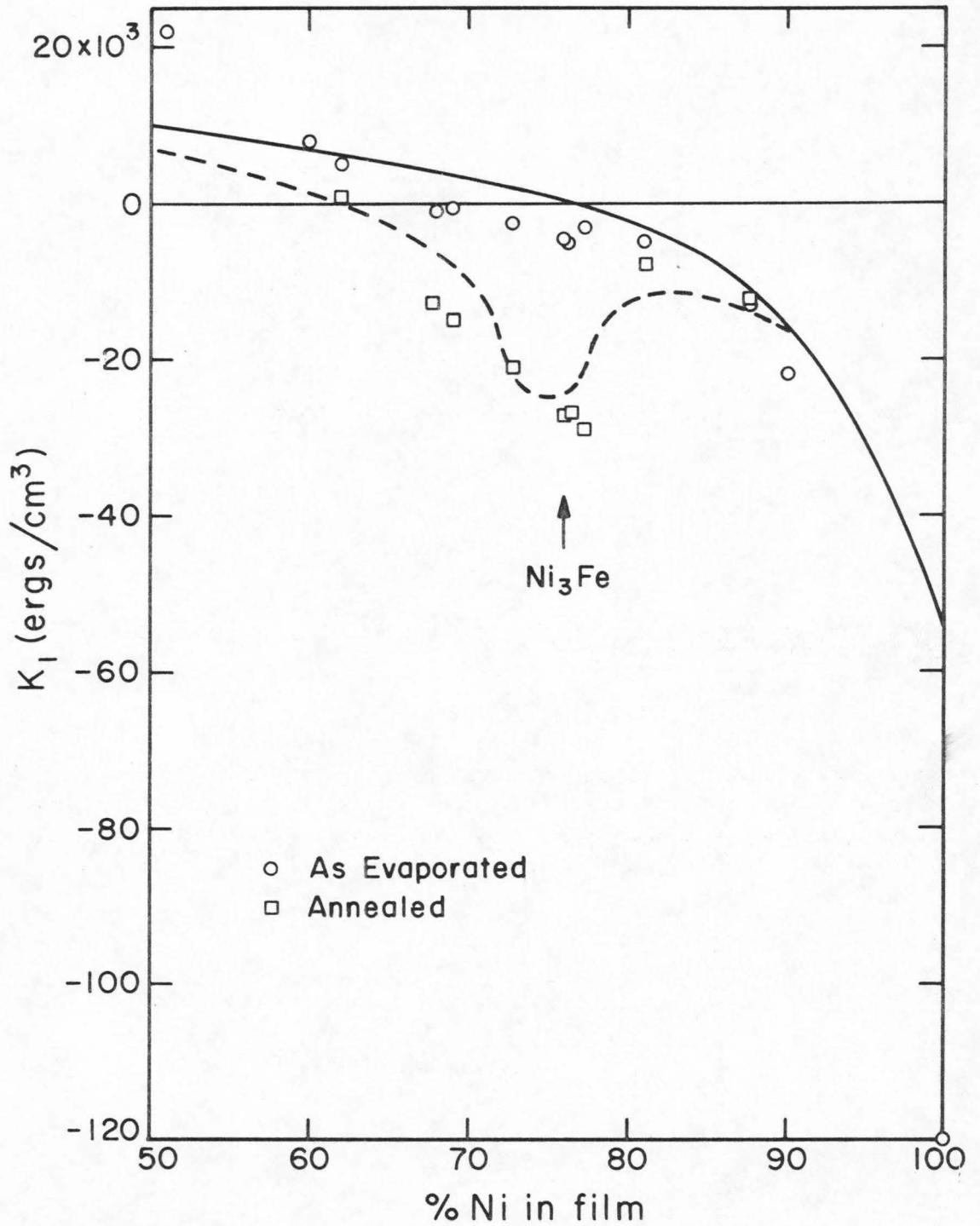


Fig. 3-3 Measured values of magnetocrystalline anisotropy before and after annealing vs. weight percentage composition. The solid and dashed lines show disordered and ordered bulk data, respectively.

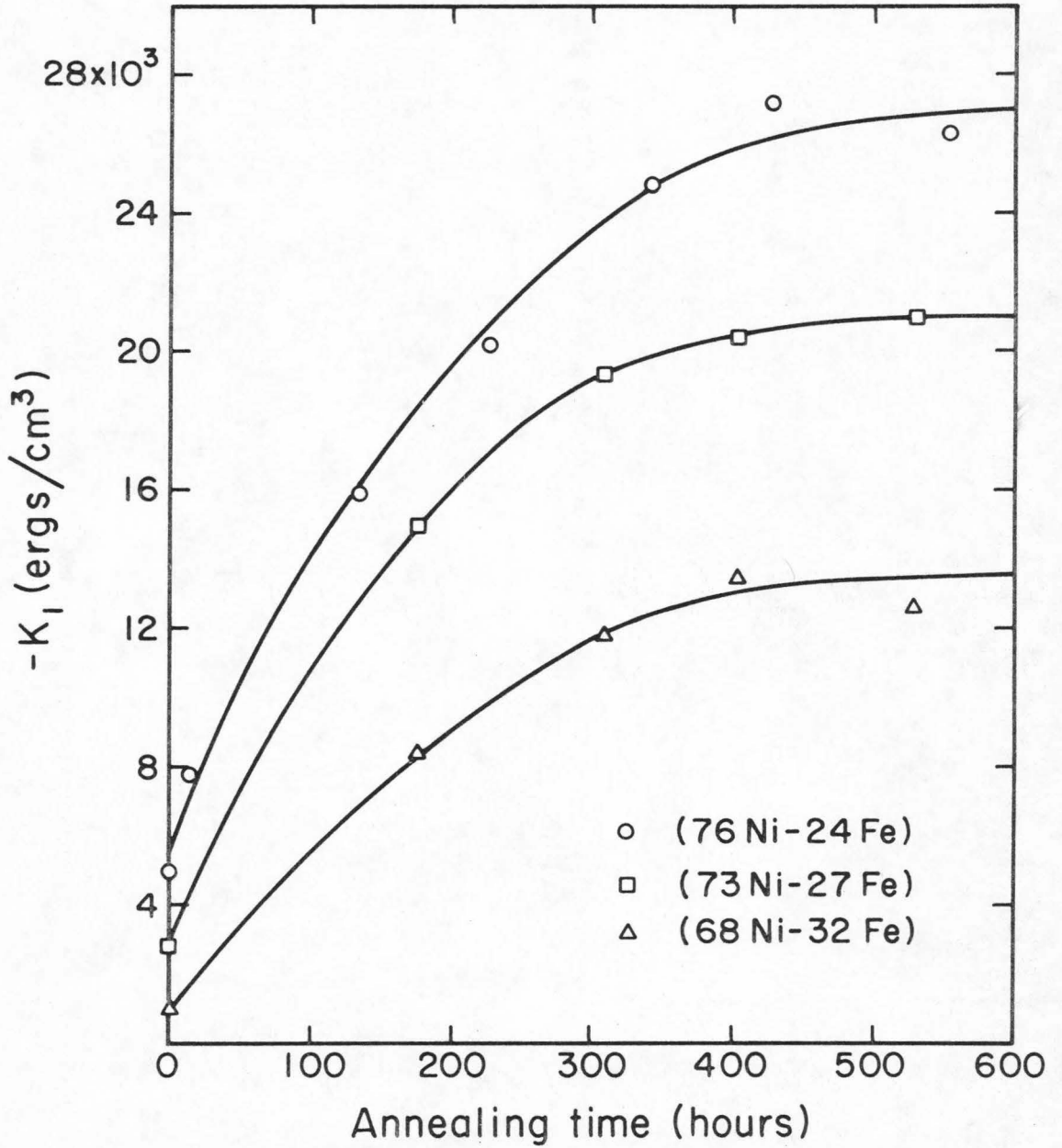


Fig. 3-4 Measured values of magnetocrystalline anisotropy vs. annealing time at three representative compositions.

values is good except at 50 Ni and 100 Ni.

#### 3.4.3 Effect of Ordering on Strain Sensitivity

Strain sensitivity measurements have been made on epitaxial films on MgO and polycrystalline films on glass before and after annealing to produce order. In Figs. 3-5 and 3-6 the measured values of strain sensitivity in the [100] and [110] directions are shown for ordered and disordered epitaxial films. All the ordered samples were annealed for at least 350 hours at 400°C. Except the 76 Ni composition, the data in both figures for ordered and disordered samples were from measurements made on a single film before and after annealing. The pairs of data points at 76 Ni were from measurements of two films evaporated at the same time but only one of which was subsequently annealed.

The solid and dashed lines in Figs. 3-5 and 3-6 are the values of strain sensitivity for disordered and ordered bulk material, respectively, calculated from Eqs. (3.6) and (3.7) using bulk data. The elastic constant data are from Einspruch and Claiborne (1964) and the bulk single crystal magnetostriction data for disordered and ordered specimens are from Bozorth and Walker (1953). The saturation magnetization data given in Bozorth (1951) are only for disordered alloys, so the percentage change in saturation magnetization with ordering as a function of composition was taken from data by Grabbe (1940).

The strain sensitivity data for polycrystalline films on glass are shown in Fig. 3-7. Again all data on ordered samples were taken after annealing the films for at least 350 hours. Except at 76 Ni, the pairs of data points were from measurements on the same film before and

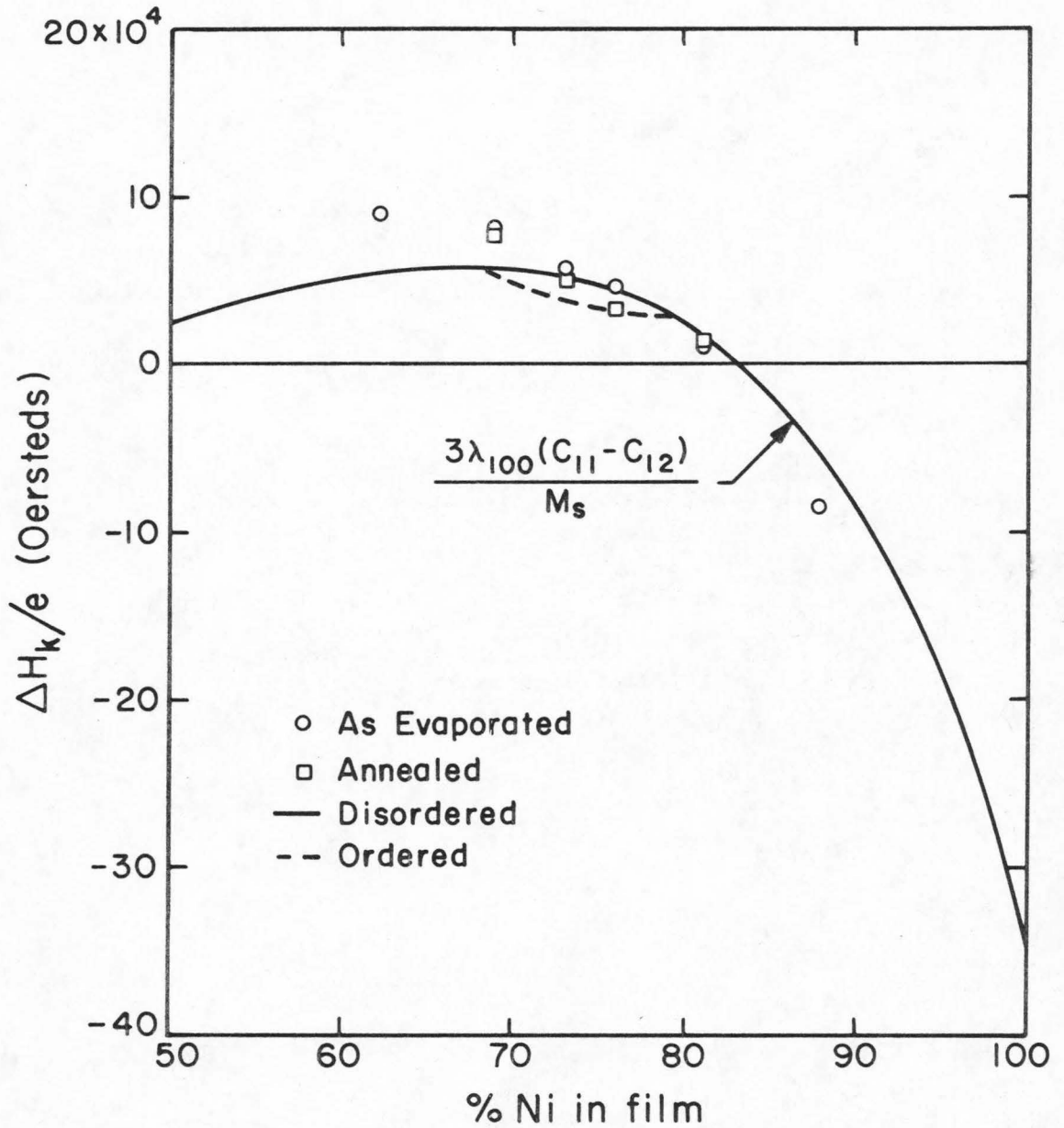


Fig. 3-5 Strain sensitivity of epitaxial Ni-Fe films for an applied strain in the [100] direction before and after annealing. The solid and dashed lines show values predicted on the basis of bulk data.

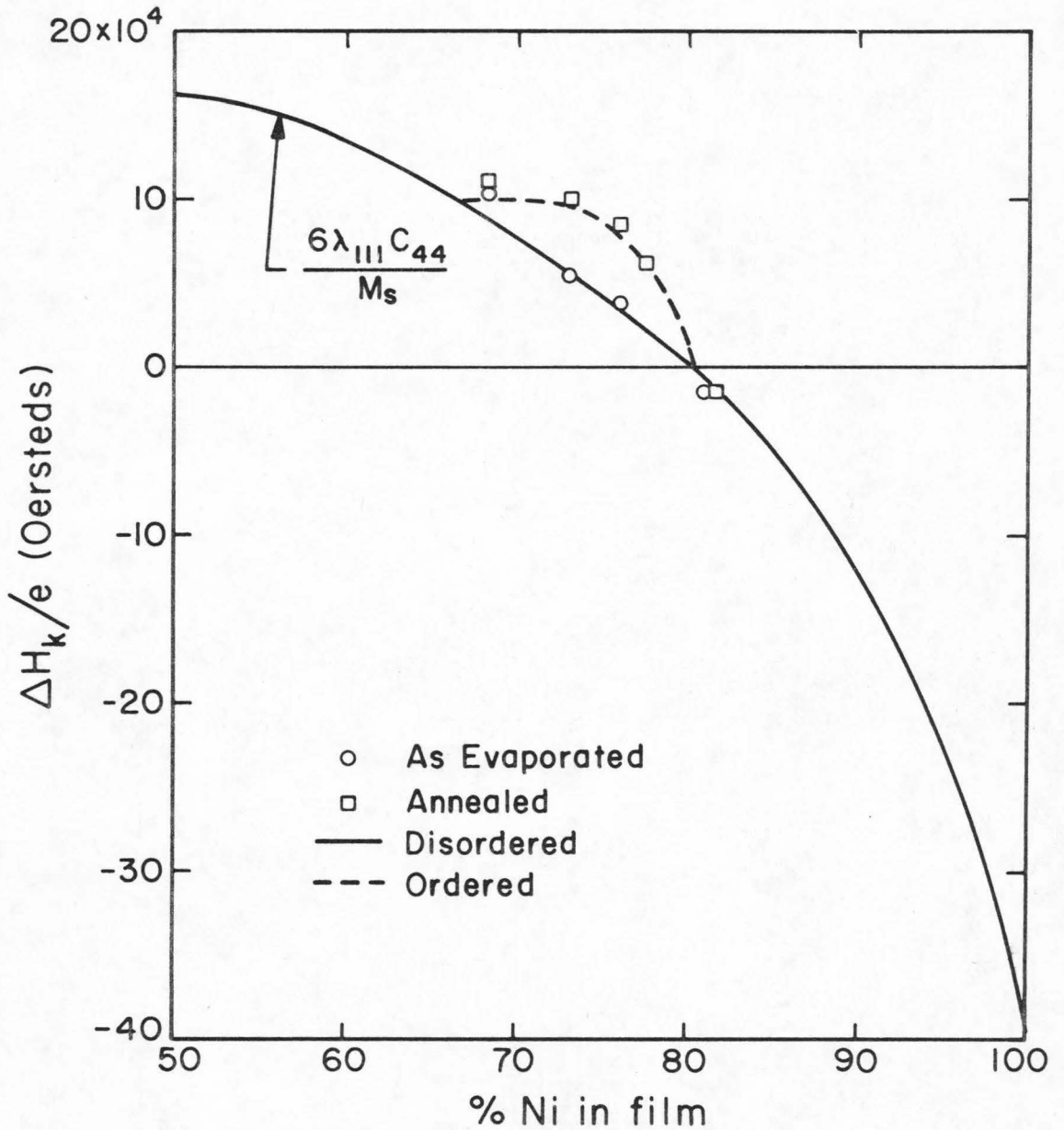


Fig. 3-6 Strain sensitivity of epitaxial Ni-Fe films for an applied strain in the [110] direction before and after annealing. The solid and dashed lines show values predicted on the basis of bulk data.

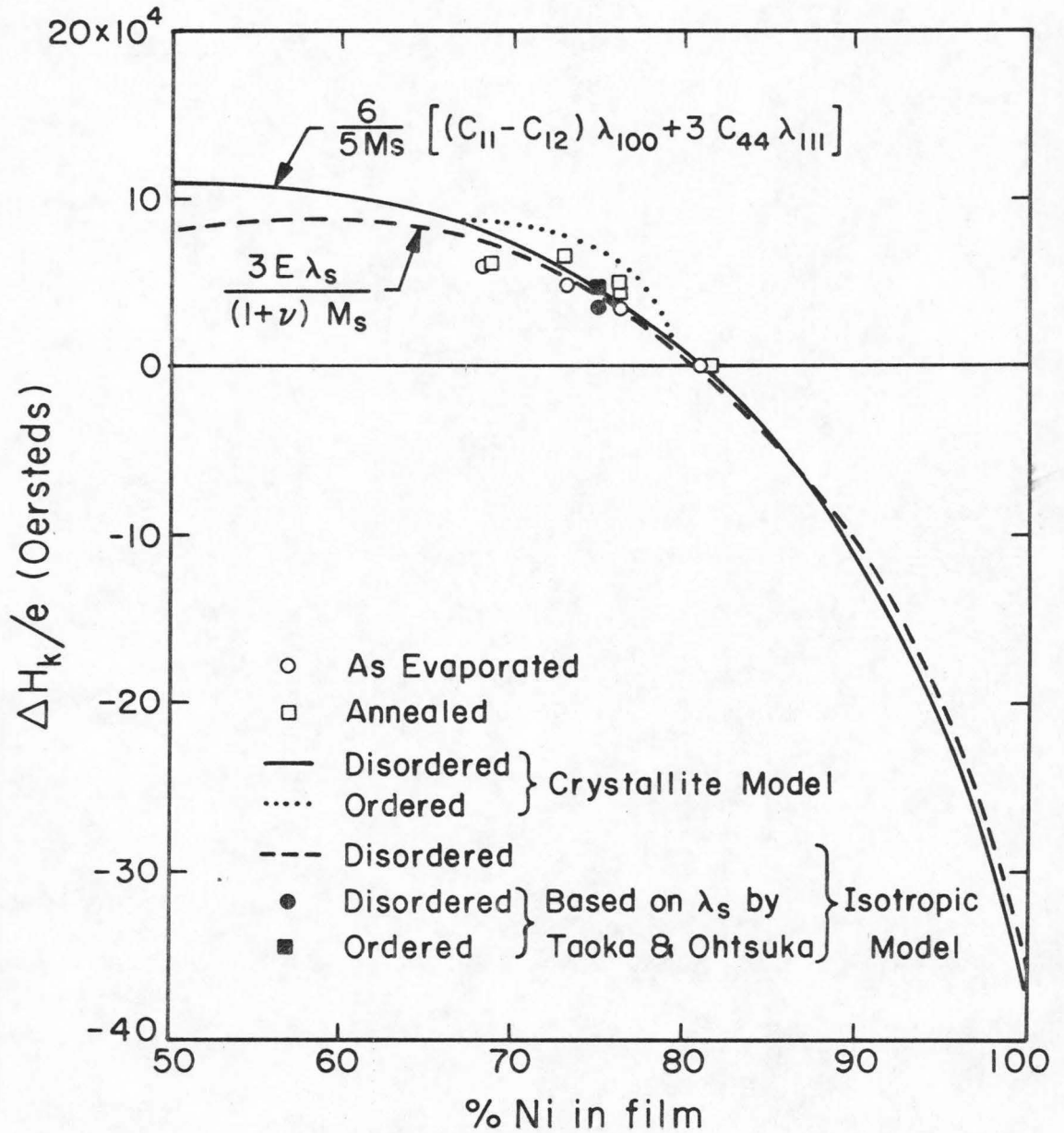


Fig. 3-7 Strain sensitivity of polycrystalline Ni-Fe films for a uniform strain before and after annealing. Predictions based on bulk data are shown for both the isotropic material model and a crystallite averaging model.

after annealing. In this case the data at 76 Ni were from three films made in three separate evaporations. Two of the films were annealed before measurement.

In the polycrystalline case the experimental strain sensitivity data is compared with the predictions of both the isotropic material model (Eq. (3.10)) and the crystallite model (Eq. (3.12)). The dashed line in Fig. 3-7 is the prediction of the isotropic material model for the disordered alloy. The saturation magnetostriction  $\lambda_s$  for disordered alloys is given by Bozorth (1951), and Young's modulus  $E$  and Poisson's ratio  $\nu$  are given by Marsh (1938). No data are available in Bozorth for the magnetostriction in ordered alloys; however, Taoka and Ohtsuka (1954) have reported a 40% increase in the saturation magnetostriction after annealing a bulk 74.9 Ni-25.1 Fe sample. The value increased from  $7.1 \times 10^{-6}$  to  $10.1 \times 10^{-6}$ . Using these values for  $\lambda_s$  in the isotropic material prediction gives two isolated points in the figure. The change in strain sensitivity predicted agrees quite well with the observed changes.

In order to calculate the predictions of the averaged crystallite model, the same bulk single crystal data as referenced earlier may be used. The solid line in Fig. 3-7 shows the predicted values for disordered alloys and the dotted line the predicted values for the ordered alloys. The predicted changes in strain sensitivity using this model also agree quite well with the observed values.

### 3.5 Discussion

The optimum annealing temperature was chosen by observing changes

in  $K_1$ . Degrees of ordering could be produced by annealing at temperatures of 450°C or higher, but maximum changes in  $K_1$  were observed after annealing at temperatures between 400° and 410°C. The ordering process was significantly slower at an annealing temperature of 390°C. In bulk specimens the order-disorder transformation temperature has been taken as 490°C. According to the present study the transformation temperature is not sharply defined with degrees of partial order being in equilibrium at temperatures between 410° and 490°C and almost complete order being the stable state at temperatures up to 410°C.

In Fig. 3-3 the apparent trend of the  $K_1$  values for unannealed samples near the  $Ni_3Fe$  composition to lie below the disordered bulk values may be due to a small degree of ordering in the samples. After the samples were evaporated onto the heated substrates, it required several minutes to cool down. This is in contrast to the quenching of bulk samples in a few seconds after being heated above 490°C. On the other hand the thin film samples were evaporated on substrates maintained at 325° to 335°C. At these temperatures the ordering process should be very slow. The explanation may be that the atoms striking the surface during deposition have a higher mobility than atoms which are already in a lattice. This could not be studied further at this time because of the inability to quench the samples in the vacuum system.

As can be seen in Fig. 3-7, the isotropic material model and the crystallite model give nearly the same predictions for the strain sensitivities in the Ni-Fe alloys between 65 Ni and 81 Ni. This makes

it difficult to determine which theoretical model best describes the real situation. Brownlow and Wilts (1971) give data on the strain sensitivities of disordered polycrystalline films over wider composition ranges in both the Ni-Fe and Ni-Co alloy systems. This makes it possible to compare the theoretical predictions of both models with experimental results over wide composition ranges in two alloys. The experimental data of Brownlow and Wilts for samples deposited on glass at 400°C are reproduced in Figs. 3-8 and 3-9 (Note that the present data for unannealed films in Fig. 3-7 are in excellent agreement with the data in Fig. 3-8). The predictions of both theoretical models are also shown. Both models give relatively good agreement with the experimental values in the Ni-Fe system. In the Ni-Co system the isotropic material model gives better agreement with the observed values especially in the region where the experimental strain sensitivity is zero. The Ni-Co alloys provide a much more stringent test for the crystallite averaging method because the theoretically predicted zero occurs when two large terms of opposite sign cancel. This is caused by the fact that the magnetostriction constants,  $\lambda_{100}$  and  $\lambda_{111}$ , for Ni-Co are not both close to zero at any given composition. In the case of Ni-Fe both  $\lambda_{100}$  and  $\lambda_{111}$  are very small near 80 Ni-20 Fe. Both models thus predict the zero strain sensitivity in Ni-Fe at the same composition. From the data presented, the isotropic material model yields predictions of strain sensitivity for polycrystalline films which are in good agreement with observed values in the Ni-Fe and Ni-Co alloy systems. The predictions of the averaging method are not as good as those of the isotropic

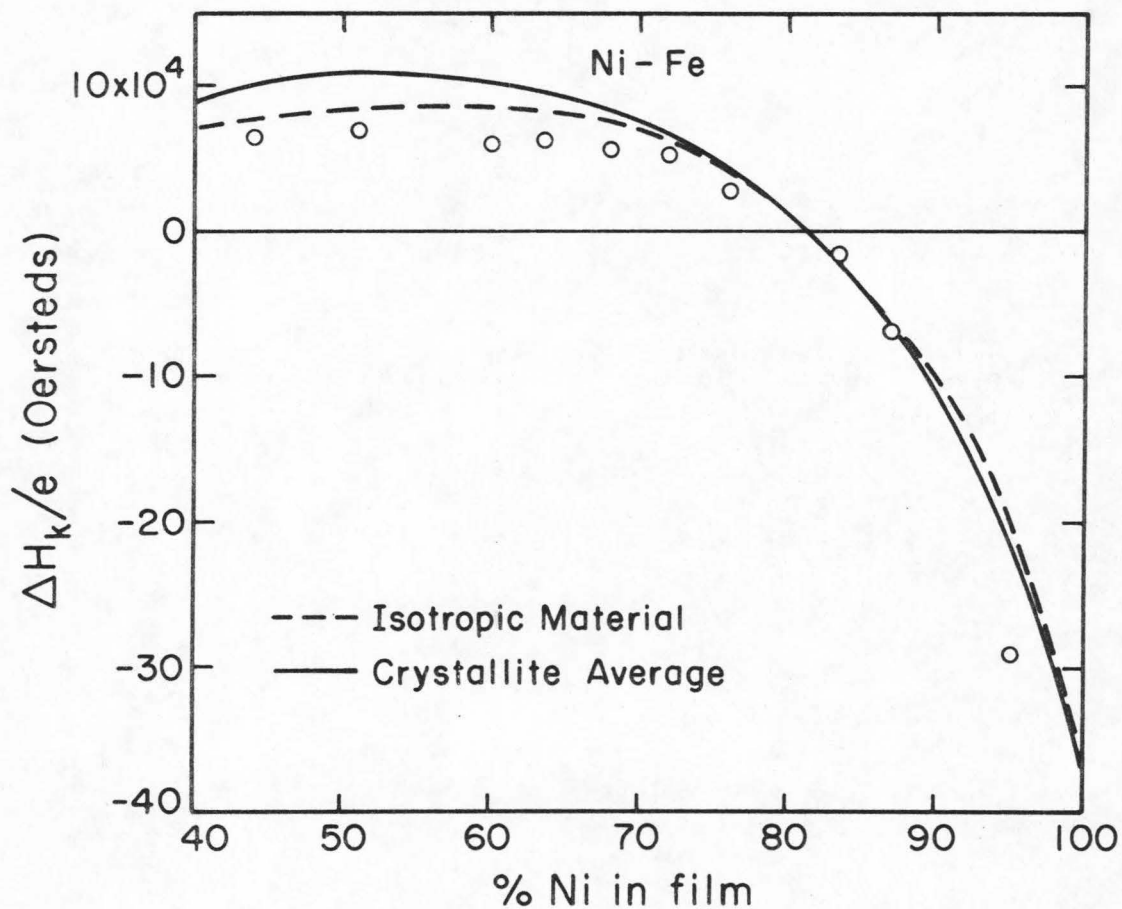


Fig. 3-8 Strain sensitivity of polycrystalline Ni-Fe films evaporated at 400°C according to Brownlow and Wilts (1971). The predictions based on bulk data of the isotropic material model and a crystallite averaging model are shown by the dashed and solid lines.

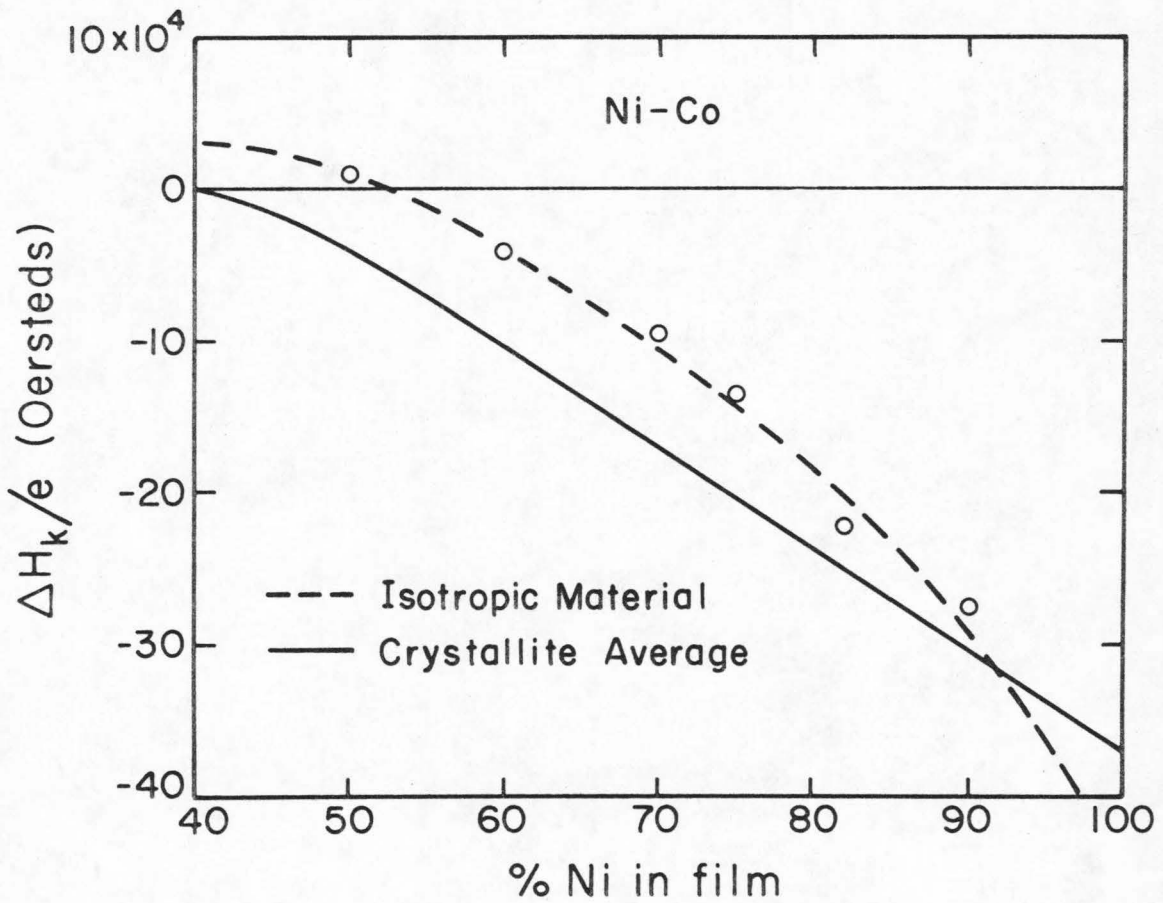


Fig. 3-9 Strain sensitivity of polycrystalline Ni-Co films evaporated at 400°C according to Brownlow and Wilts (1971). The predictions based on bulk data of the isotropic material model and a crystallite averaging model are shown by the dashed and solid lines.

material model, but the deviations are not large.

All bulk data for the Ni-Fe alloys used in calculating the theoretical curves in Fig. 3-8 have been referenced previously. For the Ni-Co alloys, Young's modulus  $E$  has been given by Yamamoto and Taniguchi (1955) and saturation magnetostriction  $\lambda_s$  by Bozorth (1951). Poisson's ratio  $\nu$  was assumed to be independent of composition with a value of 0.3 which is the value given by Marsh (1938) for pure Ni. The single crystal magnetostriction constants,  $\lambda_{100}$  and  $\lambda_{111}$ , have been given by Yamamoto and Nakamichi (1958) and the elastic constants by Leamy and Warlimont (1970).

The experimental results of this chapter show that properties of thin Ni-Fe films which can be annealed to produce the ordered  $\text{Ni}_3\text{Fe}$  phase are in satisfactory agreement with similar measurements on bulk specimens. Using methods developed in this study, it may be possible to study the process of ordering in less well known alloy systems such as Ni-Co. In this system the existence of the ordered  $\text{Ni}_3\text{Co}$  structure has never been confirmed. X-ray studies of the lattice parameter of Ni-Co alloys have given hints of its existence (Taylor, 1950), but other studies should be made.

## Chapter 4

## EFFECT OF ORDERING ON THE EXCHANGE CONSTANT A

4.1 Introduction

Ferromagnetic materials are characterized by the parallel alignment of the magnetic moments at temperatures below a critical temperature called the Curie temperature. A special kind of coupling exists between the magnetic moments causing them to line up in parallel directions by overcoming the randomizing effect of thermal motion. This coupling is called the exchange interaction and may be characterized by an exchange constant which is a quantitative measure of the strength of the interaction. It is strictly a quantum mechanical effect, having no analog in classical physics. Above the Curie temperature the thermal energy finally dominates and the ferromagnetic material becomes paramagnetic with random directions of the magnetic spins in the absence of an external field. Qualitatively this implies that a material with greater exchange coupling will also have a higher Curie temperature.

The exchange coupling for a given atom is very dependent on the local environment. In a crystal lattice the exchange coupling will be primarily a function of the nearest neighbor atoms and the lattice parameter. Any process which causes a change in the distribution of the nearest neighbors or causes a deformation of the lattice can affect the exchange coupling. As discussed in Sec. 3.1 the formation of the ordered structure  $\text{Ni}_3\text{Fe}$  changes the nearest neighbor environments of the constituent Ni and Fe atoms. In addition Wakelin and Yates (1953) found

that the lattice parameter as measured by X-ray diffraction shows a per unit decrease of  $6 \times 10^{-4}$  with ordering. Both of these effects make it plausible to expect changes in the Curie temperature and the exchange constant.

The measurement of the Curie temperature in ordered  $\text{Ni}_3\text{Fe}$  could be made in a straightforward way except for the fact that the order-disorder transformation temperature (about  $490^\circ\text{C}$  for bulk material) lies below the Curie temperature for this alloy. This makes it difficult to measure the magnetization of an ordered sample as a function of temperature up to the point where the ferromagnetic alignment disappears without causing the sample to disorder. Since the order-disorder transformation is rather sluggish, Taoka and Ohtsuka (1954) attempted to make such measurements on ordered bulk samples. They heated the samples at a rate of  $50^\circ\text{C}/\text{min}$  while measuring the magnetization and still noted what they considered to be an abrupt decrease in ordering at  $550^\circ\text{C}$ . For this reason it was concluded that the validity of the data taken on ordered samples at temperatures above  $490^\circ\text{C}$  was questionable. By use of a curve fitting method and the Weiss theoretical curve for magnetization as a function of temperature, the Curie point was estimated by extrapolation of the data taken below the order-disorder temperature. According to their data the Curie point increased from  $858^\circ\text{K}$  to  $983^\circ\text{K}$  in going from the disordered to the ordered state.

Spin wave resonance in ferromagnetic thin films was proposed over a decade ago as an excellent way of measuring the exchange constants of ferromagnetic materials. Seavey and Tannenwald (1958) were the first to observe standing spin wave modes in perpendicular ferromagnetic resonance

(the applied dc magnetic field normal to the film plane). The dispersion relation used to describe perpendicular resonance is

$$\omega = \gamma \left[ H_{a_{\perp}} - (4\pi M_s - H_{k_{\perp}}) + \frac{2Ak^2}{M_s} \right], \quad (4.1)$$

where  $\omega$  is the resonant frequency,  $\gamma$  the gyromagnetic ratio,  $H_{a_{\perp}}$  the applied dc magnetic field normal to the film plane,  $M_s$  the saturation magnetization,  $H_{k_{\perp}}$  the effective perpendicular anisotropy field,  $A$  the exchange constant, and  $k$  the wave number of the standing spin wave modes. The wave number can be written  $k = \frac{n\pi}{d}$ , where  $d$  is the film thickness and the mode number  $n$  is the number of half wavelengths through the film thickness. The values of  $n$  are determined by the boundary conditions.

In order to determine the value of  $A$  unambiguously, it is necessary to know what the appropriate boundary conditions are for the surface spins. After more than ten years there is still no consensus of opinion as to the mode identification scheme that should be used. Recently, however, a comprehensive study of spin wave resonance in 81 Ni-19 Fe films by Bajorek and Wilts (1971) indicated that a unique value of  $A$  in Eq. (4.1) could be determined by appropriately numbering the standing wave modes. They concluded that the dominant spin wave modes should be assigned even mode numbers  $n = 0, 2, 4 \dots$ . By using only the higher order modes, the value of  $A$  could then be determined from the slope of a graph of  $H_{a_{\perp}}$  as a function of  $n^2$ .

The purpose of the present study was to use ferromagnetic resonance techniques to measure the values of  $A$  for ordered and disordered samples near the  $Ni_3Fe$  composition. Since all resonance measurements

could be made at room temperature, there was no destruction of the ordering during the measurement. By using a suitable theory the observed changes in  $A$  due to ordering, if any, could be related to changes in the Curie temperature. Two possible theories, the Bloch spin wave theory and the Weiss molecular field theory, are considered. The Bloch theory gives no predicted relationship between the exchange and the Curie temperature since this theory is valid only for temperatures far below the Curie temperature.

On the other hand a semi-classical development of the Weiss molecular field theory and the consideration of only nearest neighbor interactions can be used to obtain

$$T_c = \frac{2zJS(S+1)}{3k} \quad , \quad (4.2)$$

where  $T_c$  is the Curie temperature,  $z$  the number of nearest neighbors,  $k$  Boltzmann's constant,  $J$  the exchange integral, and  $S$  the angular momentum quantum number (Kittel, 1966). In an fcc lattice the exchange integral  $J$  may also be related to the exchange constant by the equation

$$A = \frac{4JS^2}{a} \quad , \quad (4.3)$$

where  $a$  is the crystal lattice parameter (Chikazumi, 1964). Equations (4.2) and (4.3) are not strictly applicable in the case of metallic ferromagnets, since the electrons which are responsible for the resultant magnetic moments may no longer be localized at the atomic lattice sites. The saturation magnetization  $M_s$  may be expressed as  $M_s = Ng\beta\bar{S}$ , where  $N$  is the number of atoms per unit volume,  $g$  the spectroscopic splitting

factor,  $\beta$  the Bohr magneton, and  $\bar{S}$  an effective spin assumed to be localized at each lattice site. With this assumption of localized effective spins, Eq. (4.3) may be modified by the substitution of  $\bar{S}$  for  $S$ . Combining Eqs. (4.2) and (4.3), we then have

$$T_c \approx \frac{aAzN^2g^2\beta^2S(S+1)}{6kM_s^2} \quad (4.4)$$

Using the experimentally determined values of  $A$ , the Curie temperature can then be estimated.

#### 4.2 Experimental Methods

The samples were simultaneously evaporated onto Corning 0211 glass slides and evaporated epitaxially onto MgO substrates at 325°C as described previously. The annealing procedure to produce the ordered Ni<sub>3</sub>Fe structure has been discussed in Sec. 3.2. Measurements of crystal-line anisotropy  $K_1$  were made to indicate the approximate degree of order produced. The ferromagnetic resonance measurements were made using a stripline driven by oscillators ranging in frequency from 4 - 8 GHz. The magnetic field was measured with a nuclear magnetic resonance spectrometer, and the film compositions and thicknesses were determined by X-ray fluorescence.

From Eq. (4.1) it is easily seen that a plot of  $H_{a\perp}$  as a function of  $n$  for a given frequency  $\omega$  yields a straight line with a slope of  $\frac{-2A\pi^2}{M_s d^2}$ . Experimentally a straight line can only be drawn through the data for the higher order modes. Figure 4-1 shows representative plots of  $H_{a\perp}$  versus  $n^2$  for an ordered and disordered sample of 76 Ni-24 Fe composition. According to the results of Bajorek and Wilts discussed in

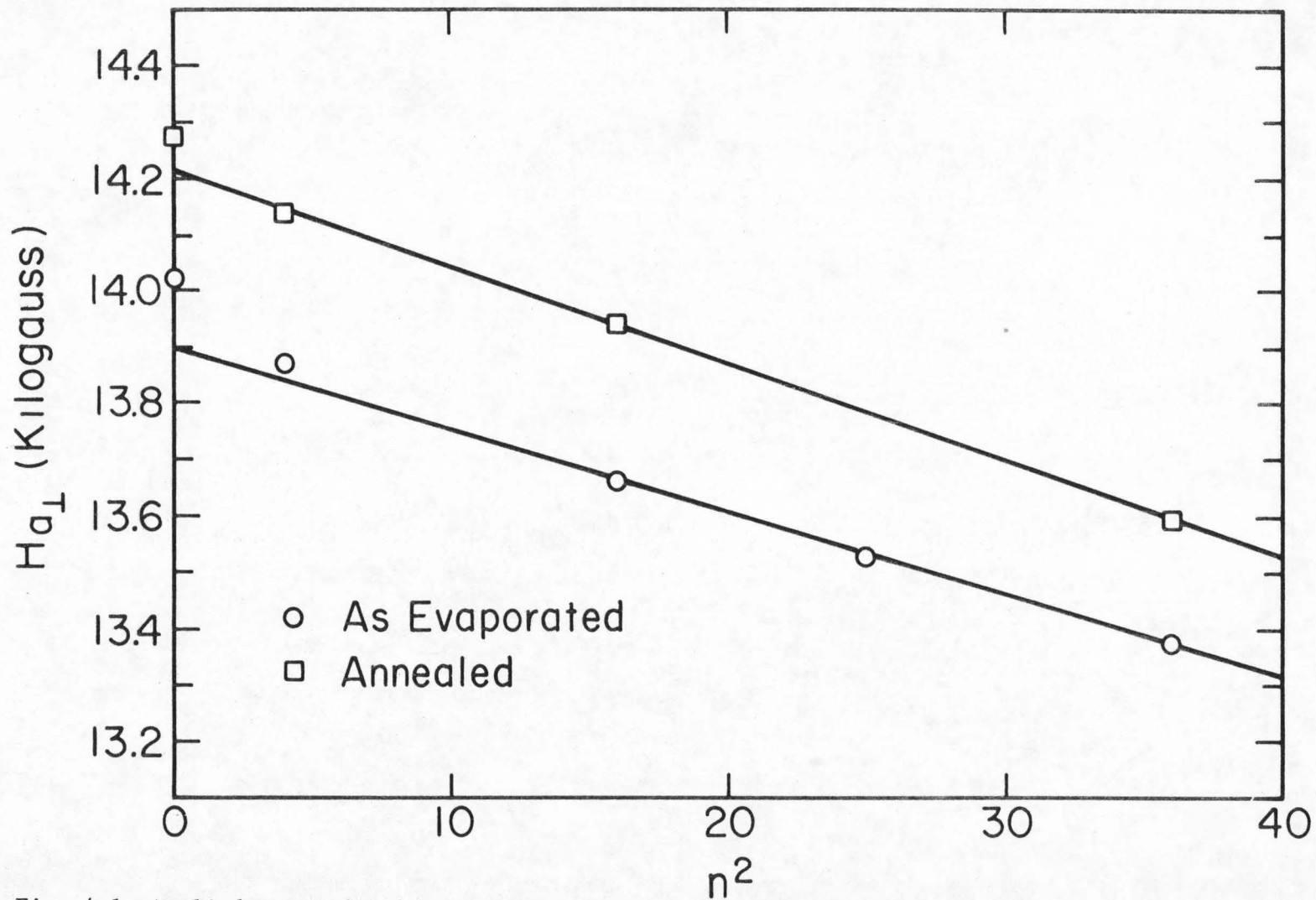


Fig. 4-1 Applied perpendicular resonance field at 7.5 GHz vs. square of spin wave mode number before and after annealing of a  $^{76}\text{Ni}$ - $^{24}\text{Fe}$  epitaxial film of thickness 3986 Å.

Sec. 4.1, the slope of the curve in Fig. 4-1 should still have the value  $\frac{-2A\pi^2}{M_s d^2}$ . Thus  $A$  may be calculated using the film thickness determined by X-ray fluorescence and the values of bulk saturation magnetization as given by Bozorth (1951). Since the values of magnetization as given by Bozorth are for disordered samples, in the case of ordered samples these values of  $M_s$  were increased by a certain percentage that was obtained from hysteresis loop tracer measurements made before and after annealing. It is also clear from Eq. (4.1) that the existence of a perpendicular anisotropy field will have no effect on the determination of  $A$ , so long as the anisotropy is independent of applied field, which is the case.

#### 4.3 Results

The measured values of the exchange constant  $A$  for epitaxial films on MgO and polycrystalline films on glass as determined by spin wave resonance are shown in Table 4.1 along with other pertinent data on each film used in this study. In Fig. 4-2 the values of  $A$  before and after annealing are shown as a function of composition. The exchange constant for unannealed samples is compared with the  $A$  values of polycrystalline films evaporated on glass at 200°C according to the data of Wilts and Lai (1972) as indicated by the dashed line in the figure. Figure 4-3 shows how the values of  $A$  changed as a function of annealing time for the same films listed in Table 4.1. From the data given it can be seen that annealing the films to produce the ordered structure increases  $A$  by 25% at Ni<sub>3</sub>Fe, by 5% at 62 Ni-38 Fe, and by about 1% at 88 Ni-12 Fe.

Table 4.1

(A in ergs/cm)

<u>Composition</u>	<u>Film Thickness</u>	<u>Before Anneal</u>	<u>After Anneal</u>	<u>Total Anneal Time</u>
62 Ni-38 Fe (Epitaxial)	4430 Å <sup>o</sup>	$1.30 \times 10^{-6}$	$1.35 \times 10^{-6}$	278 hrs.
(Polycrystalline)	4430 Å	$1.33 \times 10^{-6}$	-	-
75.8 Ni-24.2 Fe (Epitaxial)	3986 Å <sup>o</sup>	$1.05 \times 10^{-6}$	$1.31^5 \times 10^{-6}$	427 hrs.
(Polycrystalline)	3986 Å	$1.13 \times 10^{-6}$	-	-
76 Ni-24 Fe (Epitaxial)	2753 Å <sup>o</sup>	$1.08 \times 10^{-6}$	$1.35 \times 10^{-6}$	427 hrs.
(Polycrystalline)	2753 Å	$1.22 \times 10^{-6}$	-	-
88 Ni-12 Fe (Epitaxial)	3795 Å <sup>o</sup>	$0.91^4 \times 10^{-6}$	$0.92^7 \times 10^{-6}$	153 hrs.
(Polycrystalline)	3795 Å	$1.02 \times 10^{-6}$	-	-

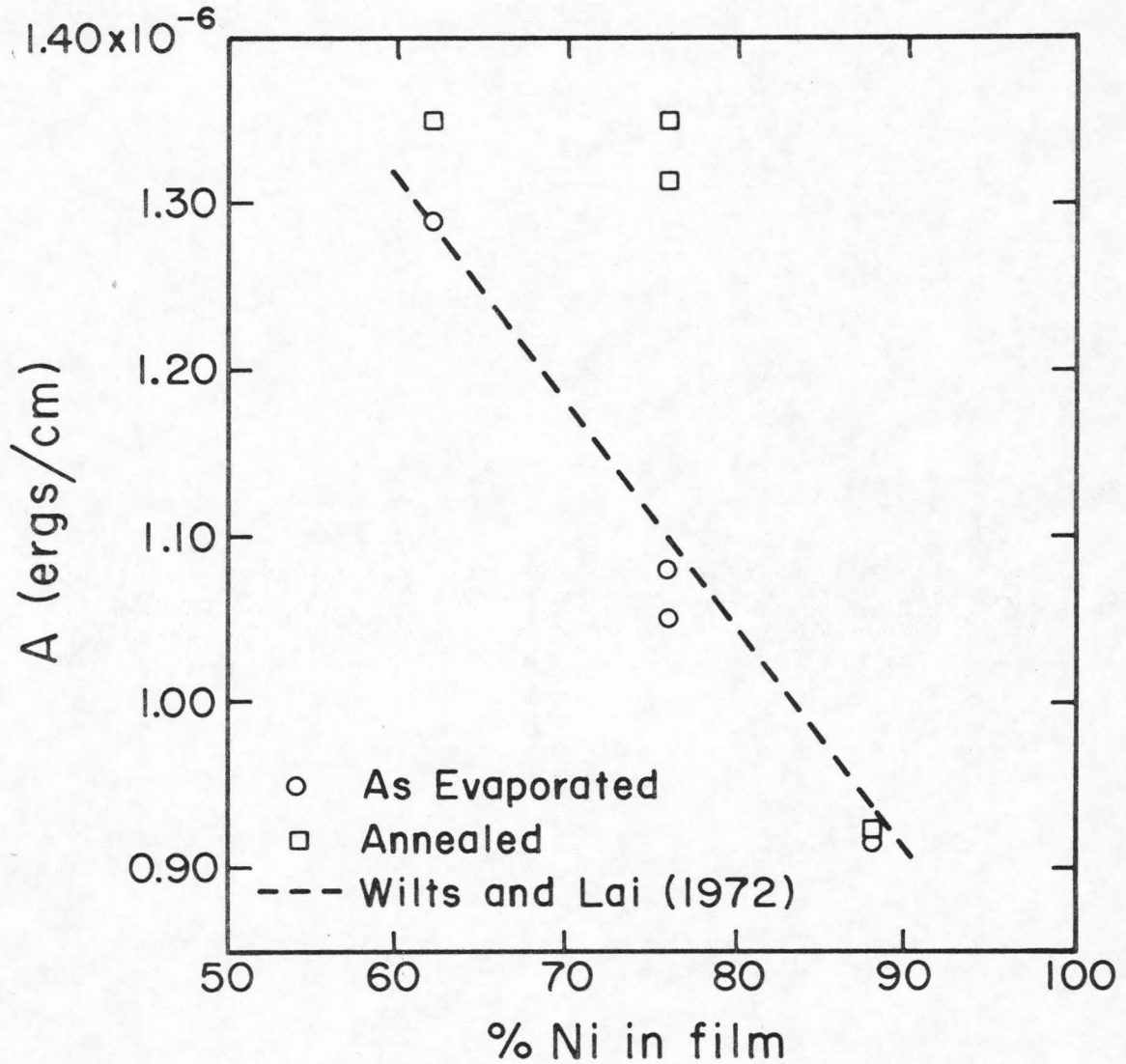


Fig. 4-2 Exchange constant  $A$  of Ni-Fe epitaxial films vs. weight percentage composition before and after annealing. The dashed line shows values of  $A$  for polycrystalline films deposited on glass substrates at  $200^{\circ}\text{C}$  according to Wilts and Lai (1972).

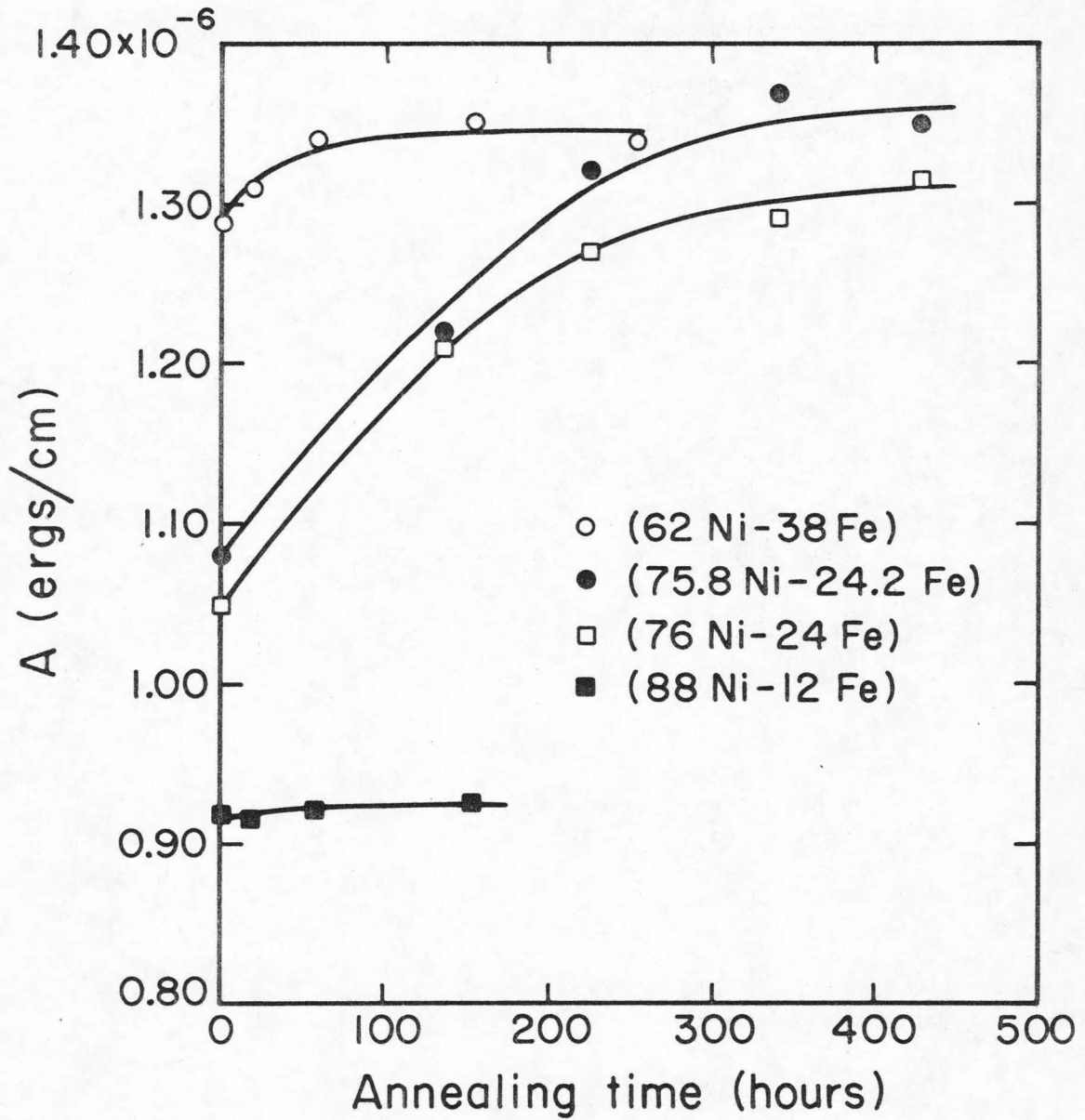


Fig. 4-3 Exchange constant  $A$  vs. annealing time for epitaxial Ni-Fe films.

#### 4.4 Discussion

Polycrystalline films on Corning 0211 glass slides were made as companion samples for each of the epitaxial films used in this study. As evaporated on glass at 325°C, both films at 76 Ni gave values of  $A$  which were 10% higher than the values of  $A$  from the corresponding epitaxial films on MgO. With subsequent annealing at 400°C the identification of the modes for the samples on glass became ambiguous and no meaningful values of  $A$  could be obtained. For this reason, no data are reported for annealed polycrystalline samples. At the present time this effect which is only seen in films on glass is not understood. As shown in Fig. 4-2 the values of  $A$  for disordered epitaxial films on MgO agree well with reported values of  $A$  for unannealed polycrystalline samples evaporated onto 0211 glass substrates at 200°C (Wilts and Lai, 1972).

Hatherly et al. (1964) have used a small-angle neutron scattering technique to measure the exchange parameter  $D$  of Ni-Fe alloys. This exchange parameter  $D$  may be related to the exchange constant  $A$  by the equation  $D = \frac{2A\hbar\gamma}{M_s}$ \*, where  $\hbar$  is Planck's constant,  $\gamma$  the gyromagnetic ratio, and  $M_s$  the bulk saturation magnetization. A sample of composition 70 Ni-30 Fe which is near to the  $Ni_3Fe$  composition was measured in the ordered state and in the disordered state. The resulting exchange parameters reportedly differed by  $10 \pm 5\%$ , but no

---

\* Some authors define  $D$  differently as  $D = \frac{2A}{M_s}$ .

data are given indicating which state gave the larger value. According to Grabbe (1940), the saturation magnetization in bulk material at this composition increases 4% in going from the disordered to the ordered phase, thus the exchange parameter data implies a 14% increase or a 6% decrease in  $A$  with ordering. A 14% increase would be consistent with the present data shown in Fig. 4-2, but the lack of more specific information as to which state gave the larger exchange parameter makes any definite conclusion impossible.

Using the experimental values of  $A$  at 75.8 Ni shown in Table 4.1 for disordered and ordered samples on MgO, we can now estimate the values of  $T_c$  by means of Eq. (4.4). It is assumed that  $S = \frac{1}{2}$ ,  $g = 2$ , and  $z = 12$  and that  $g$  and  $S$  are independent of ordering. The lattice parameter,  $3.55 \text{ \AA}$ , and the value of  $M_s$ , 890 gauss, are taken from Bozorth (1951) for the disordered alloy, but according to Grabbe,  $M_s$  is increased by 6% for the ordered structure at this composition. The values of  $T_c$  are calculated to be  $1340^\circ\text{K}$  and  $1490^\circ\text{K}$  for the disordered and ordered phases, respectively. This represents an increase of about 12% due to the ordering. According to the data of Taoka and Ohtsuka (1954), it was estimated that the Curie temperature of bulk material increased from  $858^\circ\text{K}$  to  $983^\circ\text{K}$  with ordering, an increase of about 14%. The absolute values of  $T_c$  predicted by the molecular field theory are about 50% higher than these values, but the percent change predicted is in good agreement. The only conclusion which can be made is that this rather simple theory under the assumptions given yields qualitative agreement with other estimates of the Curie

temperature change with the formation of the ordered  $\text{Ni}_3\text{Fe}$  structure.

## Appendix 1

## STRAIN SENSITIVITY OF SINGLE CRYSTALS

From the expressions given for the magnetocrystalline, elastic, and magnetoelastic energy densities in Chap. 2 (see Eqs. (2.1), (2.2), and (2.3)), it is easily seen that contributions to the magnetic uniaxial anisotropy energy density due to deformation of a cubic crystal can only arise from the magnetoelastic component. This is given by

$$E_{\text{mag-el}} = B_1 \left[ e_{11} \left( \alpha_1^2 - \frac{1}{3} \right) + e_{22} \left( \alpha_2^2 - \frac{1}{3} \right) + e_{33} \left( \alpha_3^2 - \frac{1}{3} \right) \right] \\ + B_2 [e_{12} \alpha_1 \alpha_2 + e_{23} \alpha_2 \alpha_3 + e_{31} \alpha_3 \alpha_1], \quad (\text{A-1.1})$$

where the B's may be related to the magnetostriction constants in the [100] and [111] crystal directions by the relations

$$B_1 = -\frac{3}{2} (C_{11} - C_{12}) \lambda_{100}, \\ B_2 = -3C_{44} \lambda_{111}. \quad (\text{A-1.2})$$

The  $C_{ij}$  are the elastic constants, the  $e_{ij}$  are the strain tensor components, and the  $\alpha$ 's are the direction cosines of the magnetization with respect to the cubic axes. Rewriting Eq. (A-1.1) in terms of the magnetostriction constants and keeping only angular terms, the magnetoelastic energy density becomes

$$E_{\text{mag-el}} = -\frac{3}{2} (C_{11} - C_{12}) \lambda_{100} [e_{11} \alpha_1^2 + e_{22} \alpha_2^2 + e_{33} \alpha_3^2] \\ - 3C_{44} \lambda_{111} [e_{12} \alpha_1 \alpha_2 + e_{23} \alpha_2 \alpha_3 + e_{31} \alpha_3 \alpha_1]. \quad (\text{A-1.3})$$

For a uniform strain  $e$  with direction cosines  $\beta_i$  relative to the cubic axes, the strain tensor components become

$$\begin{aligned} e_{ii} &= e\beta_i^2, \\ e_{ij} &= 2e\beta_i\beta_j \quad i \neq j. \end{aligned} \quad (\text{A-1.4})$$

Substituting Eq. (A-1.4) into (A-1.3), the anisotropy energy induced in a single crystal by a uniform strain is given by

$$\begin{aligned} E'_{K_e} &= -\frac{3}{2} (C_{11} - C_{12})\lambda_{100} e[\alpha_1^2\beta_1^2 + \alpha_2^2\beta_2^2 + \alpha_3^2\beta_3^2] \\ &\quad - 6C_{44}\lambda_{111} e[\alpha_1\alpha_2\beta_1\beta_2 + \alpha_2\alpha_3\beta_2\beta_3 + \alpha_3\alpha_1\beta_3\beta_1]. \end{aligned} \quad (\text{A-1.5})$$

For the thin film geometry it is assumed that the film is rigidly attached to the substrate and the strain induced by bending the substrate is uniform through the film thickness. The magnetization is also constrained to be in the film plane because of the large shape demagnetizing field. For a film lying in the (001) plane,  $\alpha_3$  is equal to zero, and thus  $\alpha_1$  and  $\alpha_2$  are related by  $\alpha_1^2 + \alpha_2^2 = 1$ . Applying a uniform strain in the [100] direction such that  $\beta_1 = 1$  and  $\beta_2 = \beta_3 = 0$  then gives

$$E_{K_{100}} = K_{100} \sin^2 \phi = \frac{3}{2} (C_{11} - C_{12})\lambda_{100} e \sin^2 \phi, \quad (\text{A-1.6})$$

where  $\phi$  is the angle between the magnetization and the strain. For a uniform strain applied in the [110] direction such that  $\beta_1 = \beta_2 = 1/\sqrt{2}$  and  $\beta_3 = 0$ , Eq. (A-1.5) becomes

$$E_{K_{110}} = K_{110} \sin^2 \phi = 3C_{44}\lambda_{111} e \sin^2 \phi, \quad (\text{A-1.7})$$

where  $\phi$  is again the angle between the magnetization and the applied strain. The effective uniaxial anisotropy field is given by the relation  $H_k = \frac{2K}{M_s}$ , where  $M_s$  is the magnetization, and the strain sensitivity, which is the change in effective uniaxial anisotropy field due to a uniform strain, may then be written as

$$\frac{\Delta H_{k100}}{e} = \frac{3(C_{11} - C_{12})\lambda_{100}}{M_s}, \quad (\text{A-1.8})$$

and

$$\frac{\Delta H_{k110}}{e} = \frac{6C_{44}\lambda_{111}}{M_s} \quad (\text{A-1.9})$$

for the [100] and [110] directions, respectively.

## Appendix 2

## STRAIN SENSITIVITY BASED ON ISOTROPIC MATERIAL MODEL

The induced uniaxial anisotropy energy density in a bulk polycrystalline material in a single domain state due to a uniform uniaxial stress  $\sigma$  may be written

$$E_{K\sigma} = \frac{3}{2} \lambda_s \sigma \sin^2 \phi \quad , \quad (\text{A-2.1})$$

where  $\lambda_s$  is the saturation magnetostriction constant and  $\phi$  is the angle between the applied stress and the magnetization (Bozorth, 1951). A thin film of isotropic material which is rigidly attached to a substrate may be uniformly strained in the film plane by bending the substrate. The film will then be in a condition of uniform longitudinal strain and zero transverse strain in the film plane and zero stress normal to the plane. If the x-y plane is taken to be the film plane and the z-direction is taken to be normal to the film plane, then the equations describing the behavior of the film under a uniform strain in the x-direction may be written as follows:

$$e_x = \frac{1}{E} (\sigma_x - \nu \sigma_y), \quad (\text{A-2.2})$$

$$e_y = 0 = \frac{1}{E} (\sigma_y - \nu \sigma_x), \quad (\text{A-2.3})$$

$$\sigma_z = 0 \quad , \quad (\text{A-2.4})$$

where E is Young's modulus and  $\nu$  is Poisson's ratio. From Eq. (A-2.3) the relation between the stresses may be written as

$$\sigma_y = \nu \sigma_x \quad . \quad (A-2.5)$$

By combining Eqs. (A-2.2) and (A-2.5), the following expressions for the stresses are obtained

$$\sigma_x = \frac{e_x E}{1 - \nu^2} \quad (A-2.6)$$

$$\sigma_y = \frac{\nu e_x E}{1 - \nu^2} \quad . \quad (A-2.7)$$

These expressions for uniform stress in the x and y directions may now be substituted in Eq. (A-2.1), where the angle  $\phi$  is taken to be the angle between the x-axis and the magnetization. The result is as follows:

$$\begin{aligned} E_{K_\sigma} &= \frac{3}{2} \lambda_s \sigma_x \sin^2 \phi + \frac{3}{2} \lambda_s \sigma_y \cos^2 \phi \\ &= \frac{3}{2} \lambda_s \left[ \frac{e_x E}{1 - \nu^2} \sin^2 \phi + \frac{\nu e_x E}{1 - \nu^2} \cos^2 \phi \right]. \end{aligned} \quad (A-2.8)$$

By using the identity  $\cos^2 \phi = 1 - \sin^2 \phi$ , the induced anisotropy energy due to the strain  $e_x$  may be expressed as

$$E_{K_e} = \frac{3}{2} \lambda_s \frac{e_x E}{1 + \nu} \sin^2 \phi = K_e \sin^2 \phi \quad , \quad (A-2.9)$$

where only angular dependent terms have been retained. The anisotropy field  $H_k$  is related to the anisotropy energy  $K_e$  by the equation

$$H_k = \frac{2K_e}{M_s} \quad , \quad \text{where } M_s \text{ is the magnetization. The strain sensitivity,}$$

which is the change in the uniaxial anisotropy field due to an applied

uniform strain, is then given by

$$\frac{\Delta H_k}{e} = \frac{3\lambda_s E}{(1 + \nu)M_s} \quad (\text{A-2.10})$$

## REFERENCES

- J. C. Anderson, Proc. Phys. Soc. (London) 78, 25 (1961).
- C. H. Bajorek and C. H. Wilts, J. Appl. Phys. 42, 4324 (1971).
- E. L. Boyd, IBM Journal, 116 (April, 1960).
- R. M. Bozorth, Ferromagnetism (Van Nostrand, Princeton, New Jersey, 1951).
- R. M. Bozorth and J. G. Walker, Phys. Rev. 89, 624 (1953).
- L. W. Brownlow, Ph.D. Thesis, California Institute of Technology, Pasadena, California, 1971.
- L. W. Brownlow and C. H. Wilts, J. Appl. Phys. 41, 1250 (1970).
- L. W. Brownlow and C. H. Wilts, IEEE Trans. Magnetics 7, 718 (1971).
- S. Chikazumi, Physics of Magnetism (Wiley and Sons, New York, 1964), pp. 186-189.
- S. Chikazumi, J. Appl. Phys. 32 Supp., 81S (1961).
- N. G. Einspruch and L. T. Claiborne, J. Appl. Phys. 35, 175 (1964).
- J. F. Freedman, IBM Journal, 449 (October, 1962).
- H. Fujiwara and Y. Sugita, IEEE Trans. Magnetics 4, 22 (1968).
- E. M. Grabbe, Phys. Rev. 57, 728 (1940).
- M. Hatherly et al., Proc. Phys. Soc. (London) 84, 55 (1964).
- R. W. Hoffman, Physics of Thin Films (Academic, New York, 1966), Vol. 3, pp. 219-249.
- F. B. Humphrey and A. R. Johnston, JPL Tech. Report No. 32-321, August 10, 1962.
- C. Kittel, Introduction to Solid State Physics (Wiley and Sons, New York, 1966), 3rd Edition, Chapters 14 and 15.

- J. D. Kleis, Phys. Rev. 50, 1178 (1936).
- E. Klokholm, IBM Res. Rep. RC 1508, 1965.
- E. Klokholm and J. F. Freedman, J. Appl. Phys. 38, 1354 (1967).
- T. Koikeda, S. Fujiwara, and S. Chikazumi, J. Phys. Soc. Japan 21, 1914 (1966).
- W. Köster, Z. Metallkunde 35, 194 (1943).
- H. J. Leamy and H. Warlimont, Phys. Stat. Sol. 37, 523 (1970).
- P. Leech and C. Sykes, Phil. Mag. 27, 742 (1939).
- J. S. Marsh, The Alloys of Iron and Nickel (McGraw-Hill, New York, 1938), Vol. 1, pp. 108-111.
- W. P. Mason, Phys. Rev. 82, 715 (1951).
- C. E. Patton, J. Appl. Phys. 39, 3060 (1968).
- T. G. Phillips, Proc. Roy. Soc. (London) 292, 224 (1966).
- J. Riesenfeld, AEC Tech. Rep. 39, 1965.
- M. H. Seavey, Jr. and P. E. Tannenwald, Phys. Rev. Letters 1, 68 (1958).
- C. G. Shull and M. K. Wilkinson, Phys. Rev. 97, 304 (1955).
- T. Suzuki, Ph.D. Thesis, California Institute of Technology, Pasadena, California, 1969.
- T. Suzuki and C. H. Wilts, J. Appl. Phys. 38, 1356 (1967).
- P. E. Tannenwald and R. Weber, Phys. Rev. 121, 715 (1961).
- T. Taoka and T. Ohtsuka, J. Phys. Soc. Japan 9, 712 (1954).
- A. Taylor, J. Inst. of Metals 77, 585 (1950).
- S. Tsukahara and H. Kawakatsu, J. Phys. Soc. Japan 21, 313 (1966).
- M. Yamamoto and T. Nakamichi, J. Phys. Soc. Japan 13, 228 (1958).
- M. Yamamoto and S. Taniguchi, Sci. Rep. Res. Inst. Tohoku University 7A, 35 (1955).

R. J. Wakelin and E. L. Yates, Proc. Phys. Soc. (London) B66, 221 (1953).

C. H. Wilts and S. K. C. Lai, to be published.